AD A137070

SECURITY CLASSIFICATION OF THIS PAGE

REPORT DOCUMENTATION PAGE

1a. REPORT SECURITY CLASSIFICATION: Unclassified	1b. RESTRICTIVE MARKINGS
2a. SECURITY CLASSIFICATION AUTHORITY	3. DISTRIBUTION/AVAILABILITY OF REPORT: Approved for public release; distribution unlimited.
2b. DECLASSIFICATION/DOWNGRADING SCHEDULE	
4. PERFORMING ORGANIZATION REPORT NUMBER(S)	5. MONITORING ORGANIZATION REPORT NUMBER(S): AFOSR-TR- 83-1344
6a. NAME OF PERFORMING ORGANIZATION: MASSACHUSETTS INSTITUTE OF TECHNOLOGY; 6b. OFFICE SYMBOL (If applicable)	7a. NAME OF MONITORING ORGANIZATION: AIR FORCE OFFICE OF SCIENTIFIC RESEARCH/NA
6c. ADDRESS (City, State and ZIP Code): DEPT OF AERONAUTICS & ASTRONAUTICS, CAMBRIDGE, MA 02139	7b. ADDRESS (City, State and ZIP Code): BOLLING AIR FORCE BASE, DC 20332
8a. NAME OF FUNDING/SPONSORING ORGANIZATION: AIR FORCE OFFICE OF SCIENTIFIC RESEARCH; 8b. OFFICE SYMBOL (If applicable): AFOSR/NA	9. PROCUREMENT INSTRUMENT IDENTIFICATION NUMBER: AFOSR-80-0282
8c. ADDRESS (City, State and ZIP Code): BOLLING AFB, DC 20332	10. SOURCE OF FUNDING NOS.

PROGRAM ELEMENT NO.	PROJECT NO.	TASK NO.	WORK UNIT NO.
61102F	2307	A2	

11. TITLE (Include Security Classification): SOME UNSTEADY AERODYNAMIC CHARACTERISTICS OF SEPARATED AND ATTACHED FLOW

12. PERSONAL AUTHOR(S): Dr. Eugene E. Covert, Mr. Peter F. Lorber, Ms. Carol M. Vaczy

13a. TYPE OF REPORT	13b. TIME COVERED	14. DATE OF REPORT (Yr., Mo., Day)	15. PAGE COUNT
ANNUAL	FROM 9/1/82 TO 8/31/83	AUG 31, 1983	58

16. SUPPLEMENTARY NOTATION

17 COSATI CODES		
FIELD	GROUP	SUB GR.

18. SUBJECT TERMS (Continue on reverse if necessary and identify by block number): UNSTEADY FLOW, BOUNDARY LAYERS, FLUID MECHANICS, AIRFOIL AERODYNAMICS

19. ABSTRACT (Continue on reverse if necessary and identify by block number)

Aerodynamic characteristics of separated and attached unsteady flow about a NACA 0012 airfoil have been measured for reduced frequency from 0 to 6.4 and angles of attack up to 18 deg. Results from boundary layer and near wake ensemble averaged velocity, Reynolds stress and surface pressure distributions are presented. The flow was determined to be locally two-dimensional away from the separation point (if present), within ± 1/4 span of the airfoil centerline. A convected component of the unsteady separated pressure field was identified, and the dependence on reduced frequency, angle of attack, Reynolds number and form of transition is discussed. A geometric similarity model is suggested to explain the presence of a periodic component measured for the ensemble averaged Reynolds stresses. Finally, studies of the relative importance of acoustic and upwash velocity components of the excitation are summarized.

20. DISTRIBUTION/AVAILABILITY OF ABSTRACT	21. ABSTRACT SECURITY CLASSIFICATION
UNCLASSIFIED/UNLIMITED ☒ SAME AS RPT. ☐ DTIC USERS ☐	Unclassified

22a. NAME OF RESPONSIBLE INDIVIDUAL	22b. TELEPHONE NUMBER (Include Area Code)	22c. OFFICE SYMBOL
MICHAEL S FRANCIS, Capt, USAF	202/767-4935	AFOSR/NA

DD FORM 1473, 83 APR EDITION OF 1 JAN 73 IS OBSOLETE.

Unclassified
SECURITY CLASSIFICATION OF THIS PAGE

DTIC FILE COPY

DTIC ELECTE JAN 20 1984 E D

AFOSR-TR- 83-1344

MASSACHUSETTS INSTITUTE OF TECHNOLOGY
DEPARTMENT OF AERONAUTICS AND ASTRONAUTICS
CAMBRIDGE, MA 02139

ANNUAL REPORT

Grant # AFOSR-80-0282

entitled

SOME UNSTEADY AERODYNAMIC CHARACTERISTICS OF SEPARATED AND ATTACHED FLOW

Prepared for

Air Force Office of Scientific Research
Bolling Air Force Base, DC 20332
Attn: Capt. Michael Francis

Period of Investigation: September 1, 1982 - August 31, 1983

Investigators: Eugene E. Covert
Professor of Aeronautics and Astronautics

Peter F. Lorber
Graduate Research Assistant

Carol M. Vaczy
Graduate Research Assistant

84 01 19 105

INTRODUCTION

With one notable exception, this year's activities on Grant AFOSR-80-0282 were much different than the activities of preceeding years. This fact is a simple consequence of the evolutionary nature of this program. The first few years were spent demonstrating the feasibility of the experiment and recording and evaluating velocity and pressure data to be used as the forcing function for the boundary layer itself[1,2]. During the next year the initial boundary layer data were recorded for a variety of test conditions[3]. This was a very useful and exciting period, since much of the data represented a new combination of parameters. The last year was spent largely in consolidating the data, "filling in the envelope," as it were. It was also a period of reflection, consolidation and improved understanding of both the older and the newer data, which included studies of additional features of the experiment, such as near wake velocity profiles and separated flow pressure distributions. Additional tests were also conducted to help delineate the velocity part of the unsteady forcing function from the acoustic or pressure part. In some circumstances tests were conducted either to demonstrate, say, the two-dimensionality or lack of it, on the metric surface or to confirm or reject hypotheses or explanations of various features in the data. These results will be discussed briefly below. Some interpretations of this data will also be briefly set forth.

The notable exception referred to in the opening sentence is a result of a failure to either find a suitable research student or to

hire a suitable engineer to complete the development of the floating element shear gauge. The experience from the preceeding two years suggested that unless a suitable student or engineer was available, the results were not worth the cost. This short term loss now appears to have resulted in a long term gain for two reasons. First a cheaper, more reliable method has been adapted for our use, and second we have reprogrammed the assets and improved our ability to take simultaneous data from many hot wire and pressure sensors. Such data appear to be very valuable in the region of near separation in unsteady flow.

In this report the important aspects of the last year's studies will be briefly outlined. The results of the last few years will be placed in a more general context. This discussion will lead to a discussion of some important unanswered questions and their importance.

Technical Summary

The important technical points to be discussed are as follows:*

1. The nature of the various correlation terms in unsteady flow.
2. Experimental demonstrations of the two dimensionality of the flow field.
3. Experimental delineation of acoustic effects from unsteady velocity effects.
4. Characteristics of unsteady separated flow in this experiment.

*The geometry and the detailed nature of the experimental conditions and data acquisition system are described in detail in References 2 and 3.

5. Comments on the trailing edge flow.

6. On the proposed method of measuring shear.

Results of a study of the turbulent unsteady near wake completed in the fall of 1982 are given in the attached copy of AIAA paper 83-0127.

On the nature of the several correlation terms

Recall that our signals for, say, the tangential component of velocity are defined to contain three parts (Refs. 4, 5, 6): a time mean part, a periodic but not necessarily sinusoidal part, and the part left over. Thus if u(x,t) is our measured signal, then the time mean is defined

$$\bar{u}(x_1) = \lim_{T\to\infty} \frac{1}{2T} \int_{-T}^{T} u(x,t)dt$$

Further we can take an ensemble or phase lock average

$$\langle u(x,t)\rangle = \frac{1}{N} \sum_{n=0}^{N-1} u\left(x, t + n\frac{2\pi}{\omega} + \theta\right)$$

where $0 \leq \theta \leq 2\pi/\omega$, but is constant for each average. Note then

$$\langle u(x,t)\rangle = \bar{u}(x) + \tilde{u}(x,t)$$

This equation is, in fact, the definition of the periodic part of the signal, $\tilde{u}$. The remaining term is, by definition

$$u'(x,t) = u - \langle u\rangle = u - \bar{u} - \tilde{u}$$

Note u' has two properties, by definition

$$\text{A)} \quad \lim_{T\to\infty} \frac{1}{2T} \int_{-T}^{T} u'(x,t)dt = 0$$

$$\text{B)} \quad \sum_{n=0}^{N-1} u'(x,t + n\frac{2\pi}{\omega} + \theta) = 0$$

That is to say u' has zero time mean and has zero ensemble average. We are assuming that u' corresponds to the usual turbulent velocity component that one measures in steady flow. In turbulent boundary layer theory the term <uv> is of great importance since it leads to the "Reynolds Stress" terms. Based upon the decomposition above we find

$$\langle uv\rangle = \bar{\bar{u}}\bar{\bar{v}} + \bar{\tilde{u}}\bar{\tilde{v}} + \tilde{\bar{u}}\tilde{\bar{v}} + \tilde{\tilde{u}}\tilde{\tilde{v}} + \langle\bar{u}'\bar{v}'\rangle + \langle\bar{u}'\tilde{v}'\rangle + \langle\bar{u}'\tilde{v}'\rangle + \langle\tilde{u}'\tilde{v}'\rangle + \langle u'v'\rangle$$

The time average of this term gives

$$\lim_{T\to\infty} \frac{1}{2T} \int_{-T}^{T} (uv)dt = \bar{\bar{u}}\bar{\bar{v}}' + \lim_{T\to\infty} \frac{1}{2T} \int_{-T}^{T} (\bar{\tilde{u}}\bar{\tilde{v}} + \tilde{\bar{u}}\tilde{\bar{v}} + \tilde{\tilde{u}}\tilde{\tilde{v}})dt + \lim_{T\to\infty} \frac{1}{2T} \int_{-T}^{T} (\tilde{u}\bar{v}' + u'\tilde{\bar{v}} + u'v')dt$$

But by definition $\tilde{u}$ and $\tilde{v}$ have zero mean, so

$$\overline{(uv)} = \bar{\bar{u}}\bar{\bar{v}} + \overline{\tilde{\tilde{u}}\tilde{\tilde{v}}} + \overline{u'v'} + \overline{\tilde{u}\bar{v}'} + \overline{u'\tilde{\bar{v}}}$$

The term $\tilde{\tilde{u}}\tilde{\tilde{v}}$ is non-zero because it may contain a rectification effect. Further this sort of term will appear in the left hand side of the momentum equation for each periodic velocity term (i.e. $\bar{v}\partial\tilde{u}/\partial y$,

etc.). The terms $\overline{u'v'}$ is the classic Reynolds stress term. The last two terms would seem to have a small value (random rectifications). The real issue is whether or not u' as a function of time is of finite or zero measure. In the latter case $\overline{u'\tilde{v}}$ is identically zero. In the former it should be small. According to our data terms like $\overline{u'\tilde{v}}$ and $\overline{\tilde{u}v'}$ are less than 10^{-4} of $\overline{U_g^2}$ or less than 1% of $\overline{u'v'}$.

Similarly we may take an ensemble average, subtract out the mean and end up with

$$\widetilde{uv} = \bar{u}\tilde{v} + \tilde{u}\bar{v} + \tilde{u}\tilde{v} + \tilde{u}v' + u'\tilde{v} + u'v'$$
$$= \bar{u}\tilde{v} + \tilde{u}\bar{v} + \tilde{u}\tilde{v} + \widetilde{u'v'}$$

The appearance of the non-zero term $\widetilde{u'v'}$ is a curiosity. The basic premise is that the periodic part of each term in u and v had been removed by the previous manipulation. Figure 1 shows typical values of $\widetilde{u'v'}$ across the wake layer[7]. It is definitely not zero. It was suggested by Lorber[3] that a simple geometric argument accounts for this term. To follow this argument keep in mind that u is really a function of x and y as well as time. In the unsteady boundary layer we expect each of the several thicknesses characterizing the boundary layer to vary over a cycle. It is well known that the turbulent intensity is a function of the distance from the wall. Hence the probe sees a variation in scale position (i.e., y/δ with y fixed). So since the u' and v' correspond to different heights in the boundary layer over a cycle, so $\widetilde{u'v'}$ is non-zero. Thus, there is an unsteady contribution to the Reynolds stress, at a fixed y that varies over the cycle. This

model will be discussed further below.

Experimental Demonstrations of Two-Dimensionality

The two-dimensional characteristics of the flow pattern were measured in two ways. First, pressure taps were mounted in the lateral positions ±12.5% and ±25% of chord from the mid span location at 6 chordwise locations between x/c=0.025 and 0.98[8]. Figures 2A, B, and C show the comparison of this data for attached flow. The data show the flow is locally two-dimensional. Figures 3A-C show the same kind of data when a laminar separation bubble is present near the leading edge. This separation point location can be predicted by Stratford's criteria[9] when based upon mean flow properties to within about 20% (or about 1/2% of the chordwise position). The reattachment zone is predicted by Owen and Klanfer's criteria[10] equally well. Figures 4A-C show results for massive separation of an artificially tripped boundary layer, while Figure 4D shows the mean pressure distribution with natural transition. Lack of two-dimensionality in the leading edge bubble separation has been observed by Winkleman at the U. of Maryland[11]. More important, our data shows the separation zone for the case of artificial transition is more three-dimensional than either the laminar bubble or the massive separated region.

The other procedure to test the two-dimensionality is through wake measurements. Typical data is shown in Figures 5 and 6. The conclusion is that locally, the flow is two-dimensional for at least the distance of ± one quarter span on either side of the airfoil centerline. The two regions selected, the location of the separation

bubble and the near wake, are regions where one would expect the departure from two-dimensional flow to be the largest. Hence we are confident our conclusion that the flow is essentially two-dimensional is valid.

Characteristics of Unsteady Separated Flow

In this discussion we will deal with bulk characteristics associated with separated flow. This restriction is primarily due to problems associated with measuring the details associated with unsteady separated flow. (It is likely that a computer contolled laser anemometer could track the separation point; while there is no substantiation of this conjecture on separated flow, such measurements have been made in the wake of a propeller.) Thus separation is located more or less by examination of the mean and fluctuating pressure distribution. Hence the final separation point location is known no more accurately than the distance between pressure taps. Figure 7 shows the variation of $\bar{c}_p$ vs x/c as a function of reduced frequency, k, in the fully attached case[8]. Note the high value of the peak suction pressure coefficient (-6.2), and the tendency of the mean pressure coefficient difference to approach zero at the trailing edge. Figure 8 shows the change in mean difference when separation is present on the upper surface[8]. In this case, the mean lower surface pressure coefficient is as it was before, except near the leading edge, but the mean upper surface pressure coefficient is radically transformed. Figures 9 and 10 summarize the current data on attached flow, separated flow and the boundary regions dividing the two[8]. The transition strip is #120 grit 0.125" wide at the leading edge. In these figures "dynamic

separation" implies the flow varies between attached and separated in an intermittent way as shown in Figure 11 (which is also taken from Ref. 8). The attached interval varies from 2-30 ellipse revolutions, as is also true in the separated state.

The data allows comparison of separated and attached flow for the same α, k and Reynolds number. Figure 12 shows the first harmonic of C_p as a function of x/c and Figure 13 shows the phase lag under the same conditions. The non-attached unsteady flow seems to be convected over the front 40% of the chord, and acts as if it were attached over the last 60%. This supposition is based upon a comparison of $\widetilde{C_p}$ and its phase in attached flow. At the present time it is not clear what is being convected at approximately 0.55 U_∞, in the separated flow regime. However the data (Fig. 14) suggests that whatever it is, it is roughly the same whether the boundary layer has natural or artificial transition. Figure 15 shows the variation of convected velocity with "k". This variation is consistent with that reported by Carta et al.[12]. We note too that when $\widetilde{\Delta p}$ is added to $\overline{\Delta p}$, the angle of attack at stall is increased by the unsteady process, as reported by McCrosky et al.[13].

We note the oscillating variation of term $\widetilde{C_p}$ on the upper surface over the front half of the airfoil acts as a convected process, not an acoustic process, because a change in speed of about 50% does not change the behaviour (Fig. 16).

An examination of two summary plots (Figs. 17A, B) for a range of "k's", at α=15 degrees and for natural transition shows the amplitude

and phase of the fundamental of the unsteady pressure coefficient ($\widetilde{C_p}$) varies from the leading edge to the trailing edge as follows:

k	#humps	#valleys	phase speed	comments
0.5	1	1	slow downstream, sign change at .8. Last value of the slope is slightly negative (-.08)	rises slowly, sharp drop off at TE
1.0	2	2	.14 over last 70% of chord .~0 over 1st 30%	more or less like k=.5 for front 1/2 chord, oscillation amplitude grows toward TE
2.0	3	2	0 over 1st 20% .27 over last 80%	more or less const ampl, rising slope toward TE
3.9	3	2(3)	.45 over 1st 50% ~ zero after	decreasing ampl. towards TE flat at TE
6.4	4	4	.55 over 1st 40% ~ zero or slightly negative last 60%	decreasing ampl. toward TE, rising characteristic at TE, flat at midchord

Three features stand out on this chart. The number of cycles increase with "k". The character of the distribution changes drastically with "k". For these conditions, at low "k" the amplitude increases with "k", strongly so, over the last 20% of the airfoil. There is little going on over the front of the airfoil. At higher "k" the oscillation is maximum near the leading edge and decreases as one moves aft towards the trailing edge. Further the convection

characteristic is the strongest where the fundamental amplitude of the unsteady pressure is the largest. In the case of artificial transition, the implication is a change-over from trailing edge separation at low "k" to a leading edge separation at higher "k". This dependence at high "k" is extraordinary because at high "k" the mean plus unsteady pressure gradient effects are largest at the trailing edge. Note the unsteady flow field seems to be superimposed on the relatively constant pressure mean flow field on the upper surface.

Clearly this flowfield is not understood.

Comments on Trailing Edge Conditions

The data from References 1 and 2 show the pressure difference between the upper and lower surface seems to approach zero as the trailing edge is approached. At low values of k the variation of Δp is approximately as the square root of distance from the trailing edge. As k increases the variation is more nearly linear. Examination of Figures 7 and 8 indicates the pressure difference is finite and varies smoothly as the trailing edge is approached, whether the flow is separated or not. This implies the extended Kutta condition[14]

$$\frac{1}{2}\left(u_u^2 - u_\ell^2\right) = -\frac{d\Gamma}{dt}$$

may well be applicable here. (Note here u_u is the tangential velocity, just outside the boundary layer at the upper separation point, while u_ℓ is the tangential velocity just outside the boundary layer at the separation point on the lower surface. The latter point

is nominally at the trailing edge.) For rough purposes one could argue

$$C_p = \overline{C_p} + 2\frac{\bar{u}_\ell \tilde{u}_\ell - \bar{u}_u \tilde{u}_u}{U_\infty^2} + \frac{\tilde{u}_\ell^2 - \tilde{u}_u^2}{U_\infty^2}$$

Thus the pressure difference has a part proportional to the mean, one to the fundamental frequency and as indicated by the third term, a term proportional to the second harmonic, as shown in Figure 18, for the upper surface pressures. However the fact that the second harmonic appears only near the trailing edge reduces the validity of this argument.

On the Effect of Acoustic Excitation

The effect of the noise generated from the rotating ellipse was investigated. This was accomplished by first measuring the sound pressure level at 7 locations near the airfoil. This pressure was then reproduced using a speaker. The airfoil/speaker configuration is shown in Figure 19. Many difficulties were encountered in accurately reproducing the acoustic wave characteristics, particularly at low k. Therefore only reduced frequencies of k=2.0 and 6.4 were reproduced. For these two cases the sound pressure level could not be duplicated over the entire airfoil at the same time because the amplitude decay of the pure sound wave excitation with distance was different than the combination of effects due to the rotating ellipse. Therefore three separate sound pressures were used, one corresponding to that at the leading edge, one to that at the trailing edge, and one that is somewhere in between. (This adds a large degree of uncertainty to the

validity of the results.) The surface pressure distribution and boundary layer profiles were measured and then compared to those for the airfoil/ellipse combination.

The conclusion was reached that at low values of "k" (2 or less) the acoustic part of the response is some 30 decibels below the measured pressure with wind on. At k of 6.4 the acoustic pressure level recorded on the airfoil is 5-6 db less than the wind-on measurement. Hence the threshold for effects of compressibility on the flow must lie in the neighborhood of these higher values of k. For the most part the acoustic excitation had a negligible effect on the measured boundary layer characteristics.

On the Measurement of Shear

The detailed measurement of the velocity profile shows that (in inner coordinates) there is a region where

$$\frac{u}{u_\tau} = y^+ = \frac{yu_\tau}{\nu}$$

In this region then one can measure u near the wall and find, if ν and y are known

$$u_\tau^2 = \frac{\nu u}{y} = \frac{1}{2} U_e^2 C_f$$

For our boundary layers if we can measure u at y corresponds to $y^+ = 6$ or less we can deduce C_f. Such probes are under construction and will be calibrated in known flows.

On the Relation of These Results to Other Results

Certain of these results discussed above indicate for example that the unsteady Reynolds stress term (u'v') seems to be present in all the data[4,18] in the literature, whether the data was obtained in a channel with forced excitation, or on an airfoil which is the configuration of our experiment. Lorber's geometric argument[3] seems to apply to both channel flow and our external flow. If variables such as $\langle u \rangle$ and $\langle u'v' \rangle$ depend only on distance and some thickness $\delta(t)$, such that

$$\langle u(y,t) \rangle = \langle u(y/\delta(t)) \rangle$$

$$\langle u'v'(y,t) \rangle = \langle u'v'(y/\delta(t)) \rangle \text{ , then}$$

time and space derivatives are related by

$$\frac{\partial \langle u \rangle}{\partial t} = \frac{\partial \langle u \rangle}{\partial y} - \frac{y}{\delta} \frac{d\delta}{dt} \qquad \text{and}$$

$$\frac{\partial \langle u'v' \rangle}{\partial t} = \frac{\partial \langle u'v' \rangle}{\partial y} - \frac{y}{\delta} \frac{d\delta}{dt} \quad .$$

If the mean and first harmonic are considered, so that

$\langle u \rangle (y,t) = \bar{u}(y) + \hat{u}(y)\exp(i(\omega t - \phi_u(y)))$, and

$\langle u'v' \rangle (y,t) = \overline{u'v'}(y) + \widehat{u'v'}(y)\exp(i(\omega t - \phi_{u'v'}(y)))$, time differentiation and division produce the relation

$$\frac{\widehat{u'v'}}{\hat{u}} = \frac{\dfrac{\partial \langle u'v' \rangle}{\partial y}}{\dfrac{\partial \langle u \rangle}{\partial y}} \exp(i(\phi_u(y) - \phi_{u'v'}(y))) \quad .$$

Finally, for small unsteady amplitudes and for profiles similar at each time,

$$\frac{\partial}{\partial y}\langle u'v'\rangle \tilde{=} \frac{\partial}{\partial y}\overline{u'v'} \quad \text{and} \quad \frac{\partial}{\partial y}\langle u\rangle \tilde{=} \frac{\partial}{\partial y}\bar{u} \quad , \text{ and therefore}$$

$$\frac{\widehat{u'v'}}{\hat{u}} \tilde{=} \frac{\dfrac{\partial \overline{u'v'}}{\partial y}}{\dfrac{\partial \bar{u}}{\partial y}} \exp(i\Delta\phi_{u-u'v'})$$

This relation predicts the amplitude of $\langle u'v'\rangle$ based upon $\hat{u}$, $\bar{u}$ and $\overline{u'v'}$. Also, since the left hand side is positive and real, $\langle u'v'\rangle$ and $\langle u\rangle$ must be in phase if $\partial\overline{u'v'}/\partial y$ has the same sign as $\partial\bar{u}/\partial y$ and 180° out of phase if the signs are reversed. Figure 20 shows a comparison of computations from this model and data from our experiment. References 3 and 16 provide further details and comparisons with other data, both for phase and amplitude.

A second issue here is the relation of the "Kutta Condition" in steady and unsteady flow. There are two characteristics of the airfoil associated with the Kutta condition. The first is the statement that the pressure jump is non-infinite at the trailing edge. The data which has been developed in this program shows

(1) for all attached flows $\Delta p \to 0$ at the trailing edge;

(2) for all separated flow Δp is not infinite at the trailing edge.

This aspect of the "Kutta Condition" is absolutely satisfied in every case. The second consequence of the "Kutta Condition" is to fix the value of the circulations about the airfoil. These calculations for lamina suggest a value for the circulation is

$$\Gamma = \frac{\pi c}{u_\infty} \alpha$$

This value increases linearly with the thickness ratio for an airfoil with a cusped trailing edge, and decreases with included trailing edge angle, and decreasing Reynolds number. For an 0012 airfoil the net result is that

$$C_L = (0.9)C_{L_{IDEAL}}$$

where $C_{L_{IDEAL}}$ is the zero thickness lamina value ($2\pi\alpha$)

Figure 21 shows the value of the mean C_L at $\alpha=10^o$ for two Reynolds numbers as a function of k. Two clear conclusions are reached. First C_L mean increases with Reynolds number, and second C_L increases with reduced frequency. Figure 22 shows the unsteady increment is of the order of 0.15. This represents a substantial improvement in effectiveness of developing lift on heavily loaded airfoils in unsteady flow. The improvement in the ability of an airfoil to generate lift in unsteady flow is in substantial agreement with the data in Ref. 13. This improvement comes about in spite of the great difference in the source of the unsteady flow.

These sorts of results for the lift coefficient were not unexpected. However the data on the unsteady pressure coefficient in Figs. 12-17 have yet to be explained. The variation of c_p with x/C shown there is unexpected and unexplained. (These matters are under study[15].) This confusing situation is further complicated by

data (Figs. 11, 23) which demonstrates intermittent separation in unsteady flow.

To further compound the complexity of the situation, Figure 24 shows a rough plot of our boundary layer data on a Clauser [$\Delta/\delta - \delta(G)$] plane. The steady state "self-similar" profiles are shown as flat plate, Clauser #1 and Clauser #2. The unsteady data at small α is well away from this line (although the steady data are not too far from it) lying at a value of "G" that is too high. That is, the unsteady losses exceed those expected in steady flow. As k increases, the relative size of the unsteady losses decrease. At higher α, the unsteady losses seem to be too small compared to the "self-similar" thickness. The implications here seem simple. As the Stokes layer becomes thinner with respect to the boundary layer thickness (i.e., as k increases) more and more of the boundary layer acts approximately as a quasi-steady layer. The smaller unsteady amplitudes seen at higher frequencies may also be a factor. The consequences of this are treated in Ref. 16.

Closing Remarks

At the present time, many of the characteristics of the unsteady flow field as measured in this program are unexplained. These vary from the frequency doubling at the trailing edge for low frequency separated flows to the appearance of a transition from a downstream convected process to a standing wave as one proceeds downstream following a leading edge separation. Understanding of some of these details may or may not be improved by measurement of shear at the wall under these unsteady flow conditions. In other words the primary question is which

of these characteristics are a result of this particular test configuration and which are characteristic of general unsteady flows. At the present time the results suggest that the determination of the characteristics of the separation point may be a clarifying result. Because of the detailed balance at the separation point, it is suggested that non-obtrusive instrumentation may be the only way one can obtain unbiased data under these circumstances.

Status of Research

We have met the following program goals during the last grant year.

(1) The unsteady boundary layer computer program is operational using an algebraic turbulence model. Work is continuing on a version using a three transport equation turbulence model.

(2) We have demonstrated the two-dimensional character of the flow and find it satisfactory, except possibly near the leading edge laminar separation bubble or at the separation point if transition is forced.

(3) The behavior of the unsteady turbulent near wake has been studied for a wide range of flow conditions, revealing many interesting features.

(4) In this experiment at low reduced frequencies the unsteady flow is primarily an upwash effect, and the flow behavior is like that predicted by unsteady potential flow of an incompressible fluid. At higher reduced frequencies the pressure on acoustic wave may account for up to 10% of the excitation. The boundary layer characteristics seem to be unaffected by the acoustic excitation.

(5) More of the test matrix in α, k and R_θ has been filled in for

turbulent boundary layer profiles, including measurements of <u>, <v>, <u'u'>, <v'v'> and <u'v'>.

(6) The unsteady separated flow zone has been mapped out. Although the surface pressure distribution has revealed many interesting characteristics, the details are not yet completed. (For example, we have yet to measure the motion of the unsteady separation point.)

INTERACTIONS

Seminars

Ames Research Center, Dr. S.S. Davis

University of Maryland, Dept. of Aeronautics

Royal Institute of Technology, Dept. of Mechanics, (Stockholm)

ONERA (Paris)

Dept. of Ocean Engineering, MIT

Dept. of Aeronautical Engineering, MIT (twice)

Presentations

AIAA 21st Aerospace Science Meeting, Jan. 1983

AFOSR - U. of Colorado - Seiler Hub Workshop, Aug. 1983

Thesis

Cordier, Stephane, J.; "Characteristics of an Acoustically Excited Unsteady Turbulent Layer in an Adverse Pressure Gradient." MIT S.M. Thesis, Department of Ocean Engineering, August 1983.

References

1. Lorber, P.F.; "Unsteady Airfoil Pressures Induced by Perturbation of Trailing Edge Flow." Department of Aeronautics and Astronautics, MIT, S.M. Thesis, February 1981.

2. Lorber, P.F., and Covert, E.E.; "Unsteady Airfoil Pressures Produced by Periodic Aerodynamic Interference." AIAA Journal, 20, 9, pp. 1153-1159 (1982).

3. Covert, E.E. and Lorber, P.F.; "Unsteady Turbulent Boundary Layers in Advance Pressure Gradients." AIAA paper 82-0966, to be published in AIAA Journal.

4. Parikh, P.G., Reynolds, W.C., and Jayaraman, R.; "Behavior of an Unsteady Turbulent Boundary Layer." AIAA Journal, 20, 6, pp. 769-775 (1982).

5. Simpson, R.L., Shivaprasad, B.G., and Chew, Y.T.; "The Structure of a Separating Turbulent Boundary Layer. Part 4: Effects of Periodic Freestream Unsteadiness." J. Fluid Mechanics.

6. Telionis, D.P.; "Unsteady Viscous Flows." Springer-Verlag, NY, 1981.

7. Covert, E.E., Lorber, P.F., and Vaczy, C.M.; "Measurements of the Near Wake of an Airfoil in Unsteady Flow." AIAA paper 83-0127, January 1983.

8. Covert, E.E., Lorber, P.F., Vaczy, C.M.; "Flow Separation Induced by Periodic Aerodynamic Interference." Presented at AFOSR/FJSRC/ U. of Colorado Workshop on Unsteady Separated Flows; Aug. 10-11, 1983.

9. Stratford, B.S.; as cited in Rosenhead, L., ed, Laminar Boundary Layers; Oxford University Press, Oxford, 1963, pp. 324-329.

10. Owen, P.R., and Klaufer, L.; "On the Laminar Boundary Layer Separation from the Leading Edge of a Thin Airfoil." British ARC, CP, 220 (1953).

11. Winkleman, Allen; Personal Communication; also "An Experimental Study of Mushroom Shaped Stall Cells." AIAA paper 82-0942, presented at AIAA/ASME 3rd Joint Thermophysics, Fluids, Plasma and Heat Transfer Conference, St. Louis, Missouri, June 7-11, 1982.

12. St. Hilaire, A.O., Carta, F.O., Fink, M.P., and Jepson, W.D.; "The Influence of Sweep on the Aerodynamic Loading of an Oscillating 0012 Airfoil." NASA CR-3092 (May 1979).

13. McCroskey, W.J., Carr, L.W., and McAlister, K.M.; "Dynamic Stall Experiments on Oscillating Airfoils." AIAA Journal, Vol. 14, 1, pp. 57-63, Jan. 1976.

14. Sears, W.R.; "Unsteady Motion of Airfoils with Boundary Layer Separation." AIAA Journal, Vol. 14, No. 2, pp. 216-220 (February 1976).

15. Vaczy, C.M.; "Unsteady Separated Flow Fields Around a NACA 0012 Airfoil." MIT S.M. Thesis, in preparation.

16. Lorber, P.F.; "The Turbulent Boundary Layer on an Airfoil in Unsteady Flow." MIT PhD. Thesis, in preparation.

17. Cordier, S.J.; "Characteristics on an Acoustically Excited Unsteady Turbulent Layer in an Adverse Pressure Gradient." S.M. Thesis, MIT Department of Naval Architecture and Marine Engineering, September 1983.

18. Cousteix, J., LeBalleur, J.C., and Houdeville, R.; "Response of a Turbulent Boundary Layer to a Pulsation of the External Flow With and Without Adverse Pressure Gradient." IUTAM Symposium on Unsteady Turbulent Shear Flows, Springer-Verlag, 1981.

(THIS PAGE WAS LEFT INTENTIONALLY BLANK)

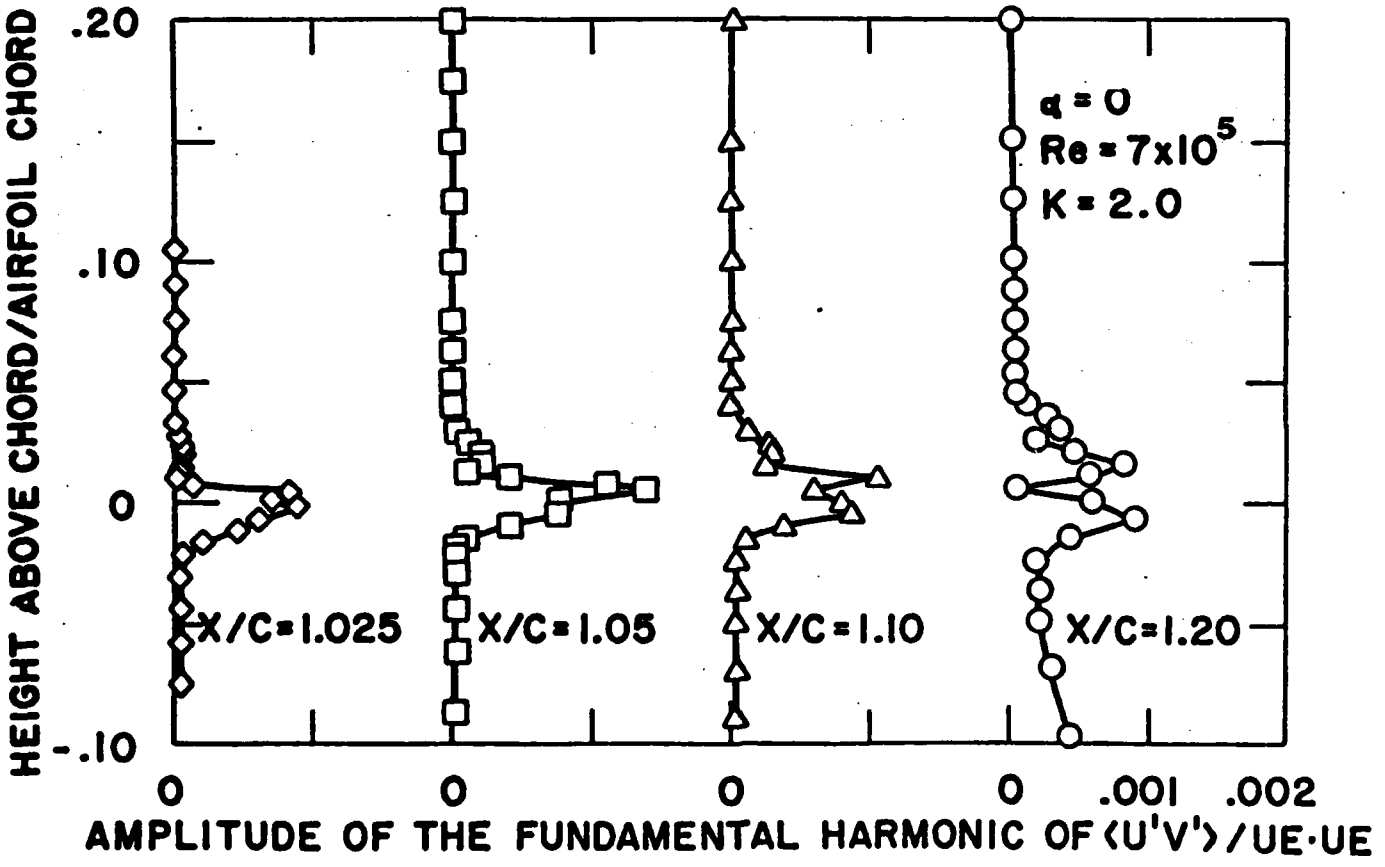

FIGURE 1: AMPLITUDE OF $\widetilde{u'v'}$ ACROSS WAKE

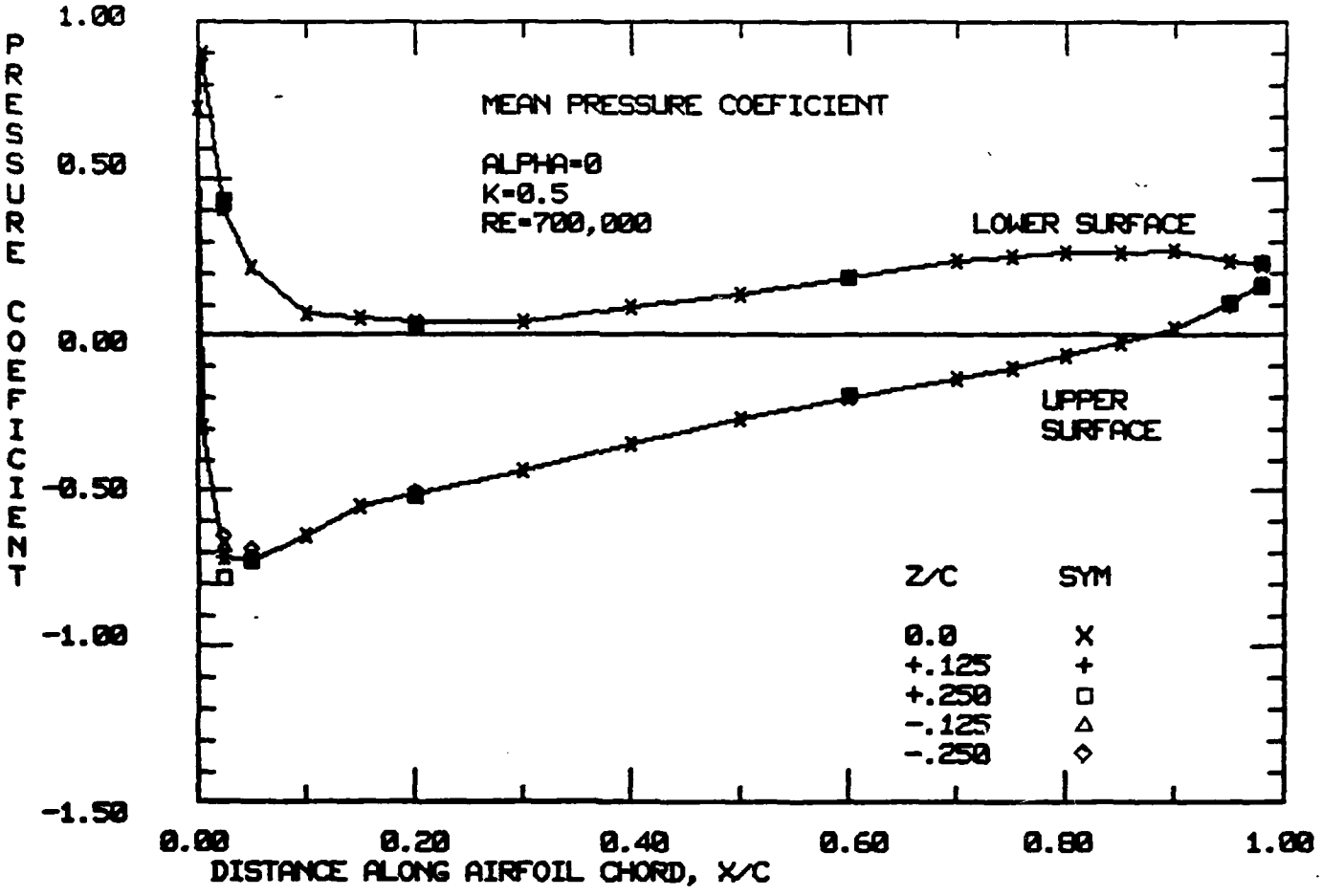

FIGURE 2A: SPANWISE DISTRIBUTION OF MEAN PRESSURE COEFFICIENT ATTACHED FLOW

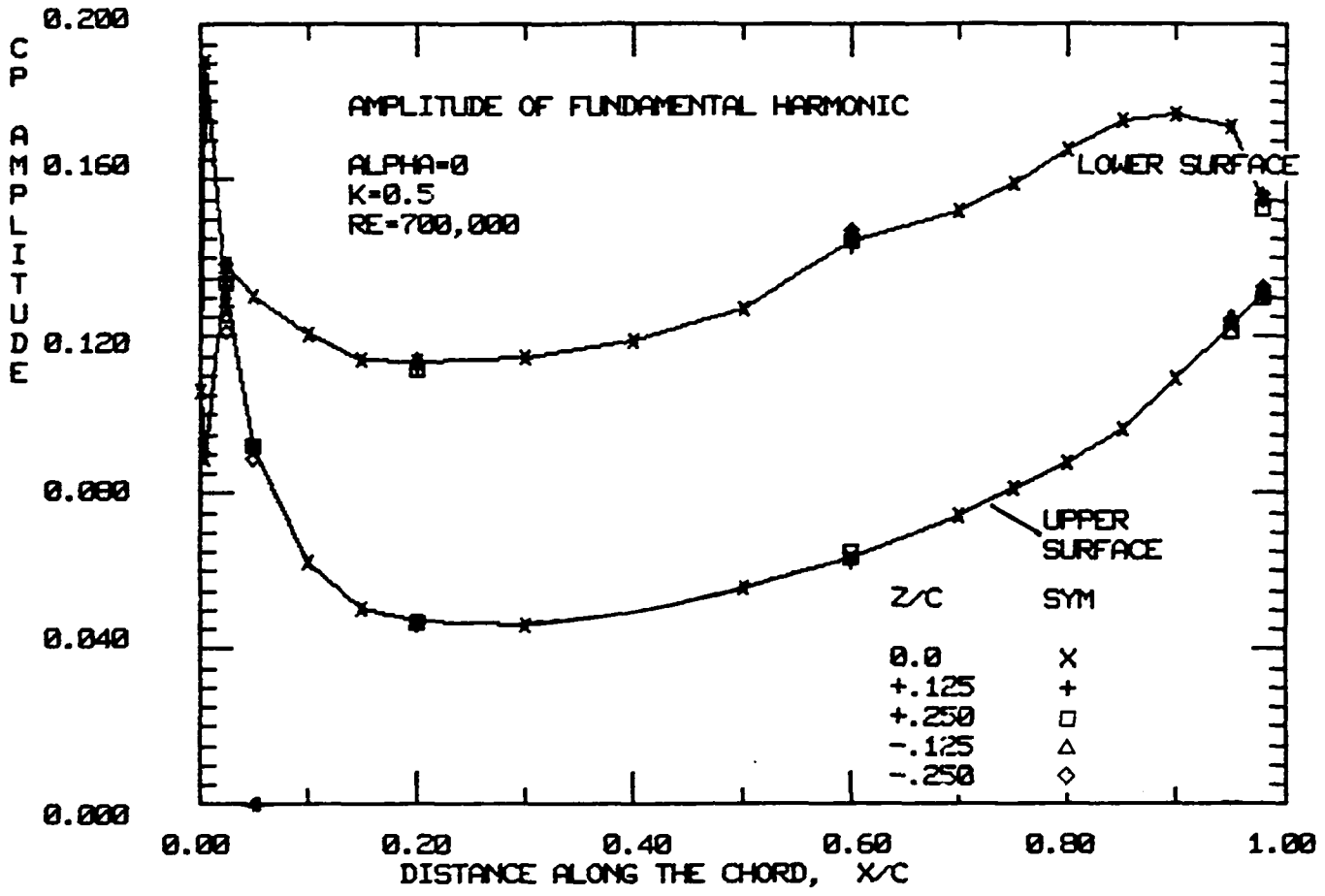

FIGURE 2B: SPANWISE DISTRIBUTION OF AMPLITUDE OF FIRST HARMONIC OF C_p

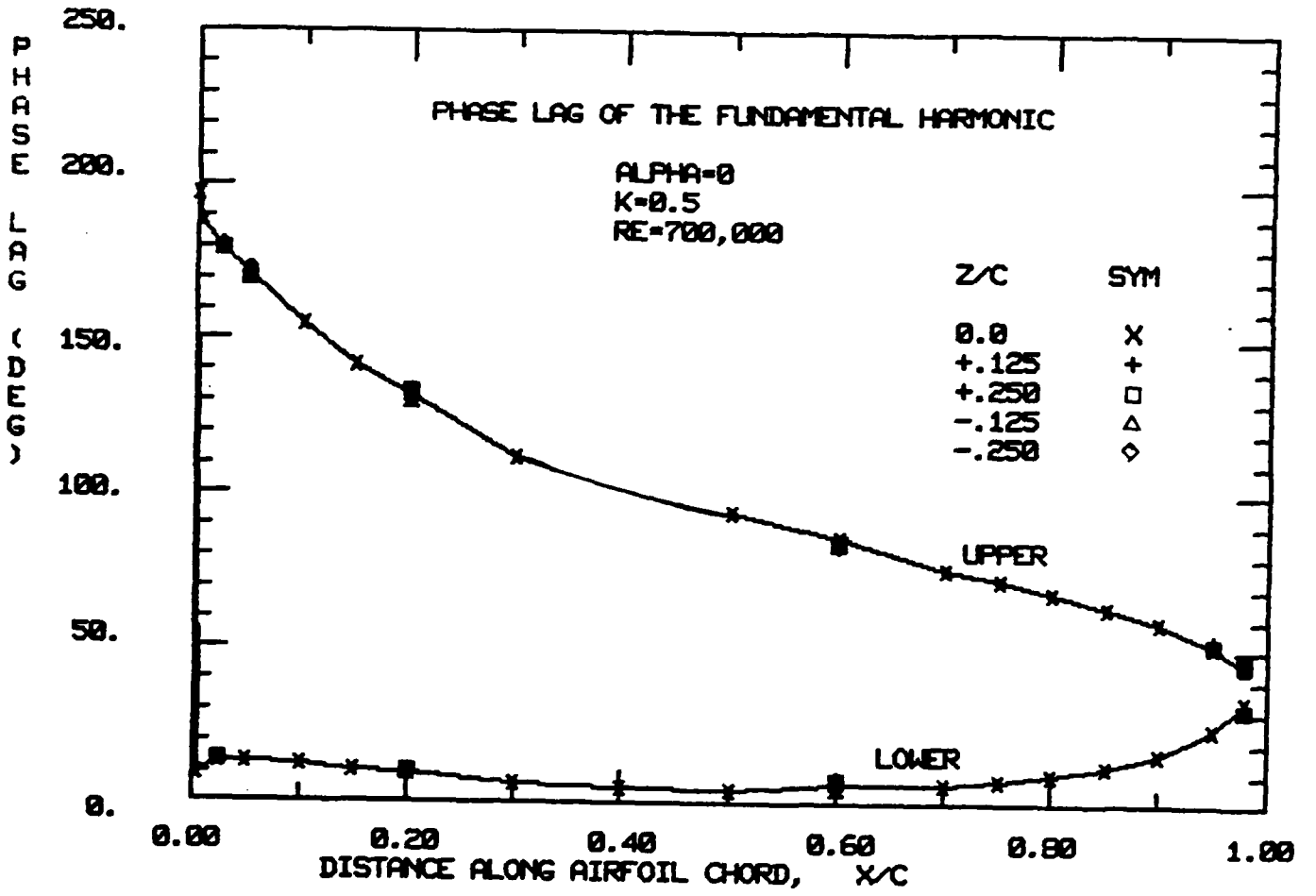

FIGURE 2C: SPANWISE DISTRIBUTION OF PHASE OF C_p

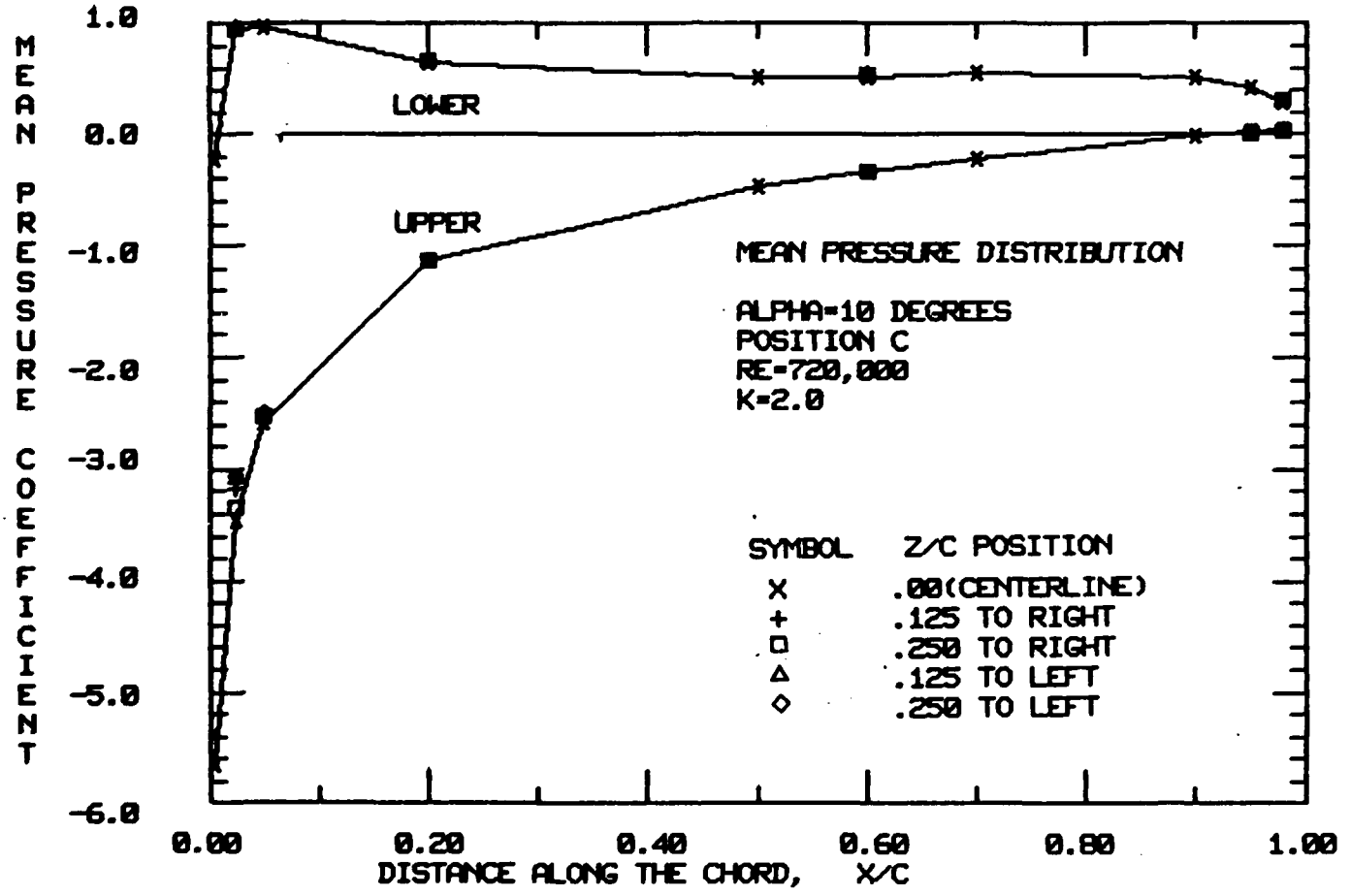

FIGURE 3A: SPANWISE DISTRIBUTION OF MEAN PRESSURE COEFFICIENT - WITH LAMINAR SEPARATION BUBBLE

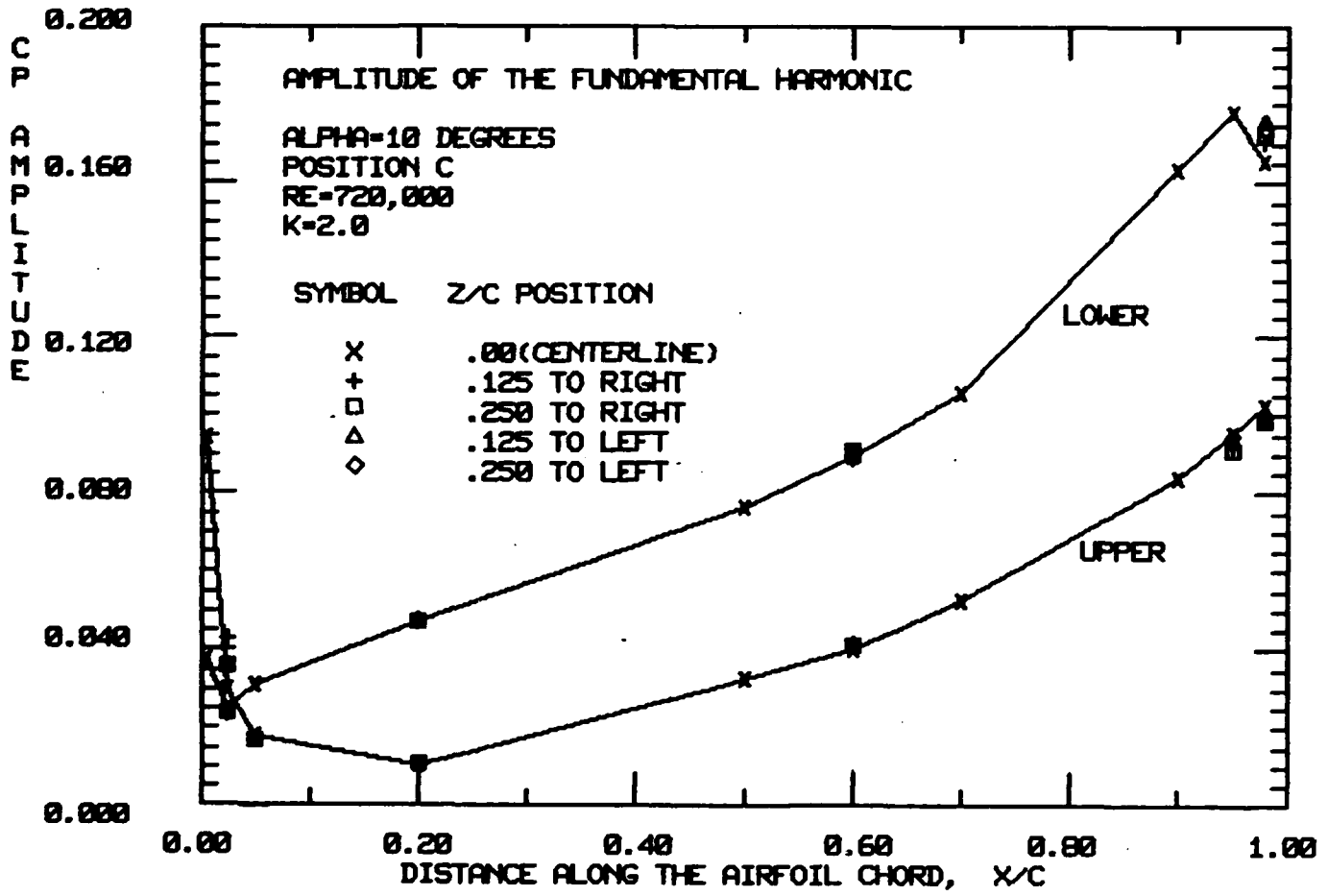

FIGURE 3B: SPANWISE DISTRIBUTION OF AMPLITUDE OF FIRST HARMONIC OF C_p - WITH LAMINAR SEPARATION BUBBLE

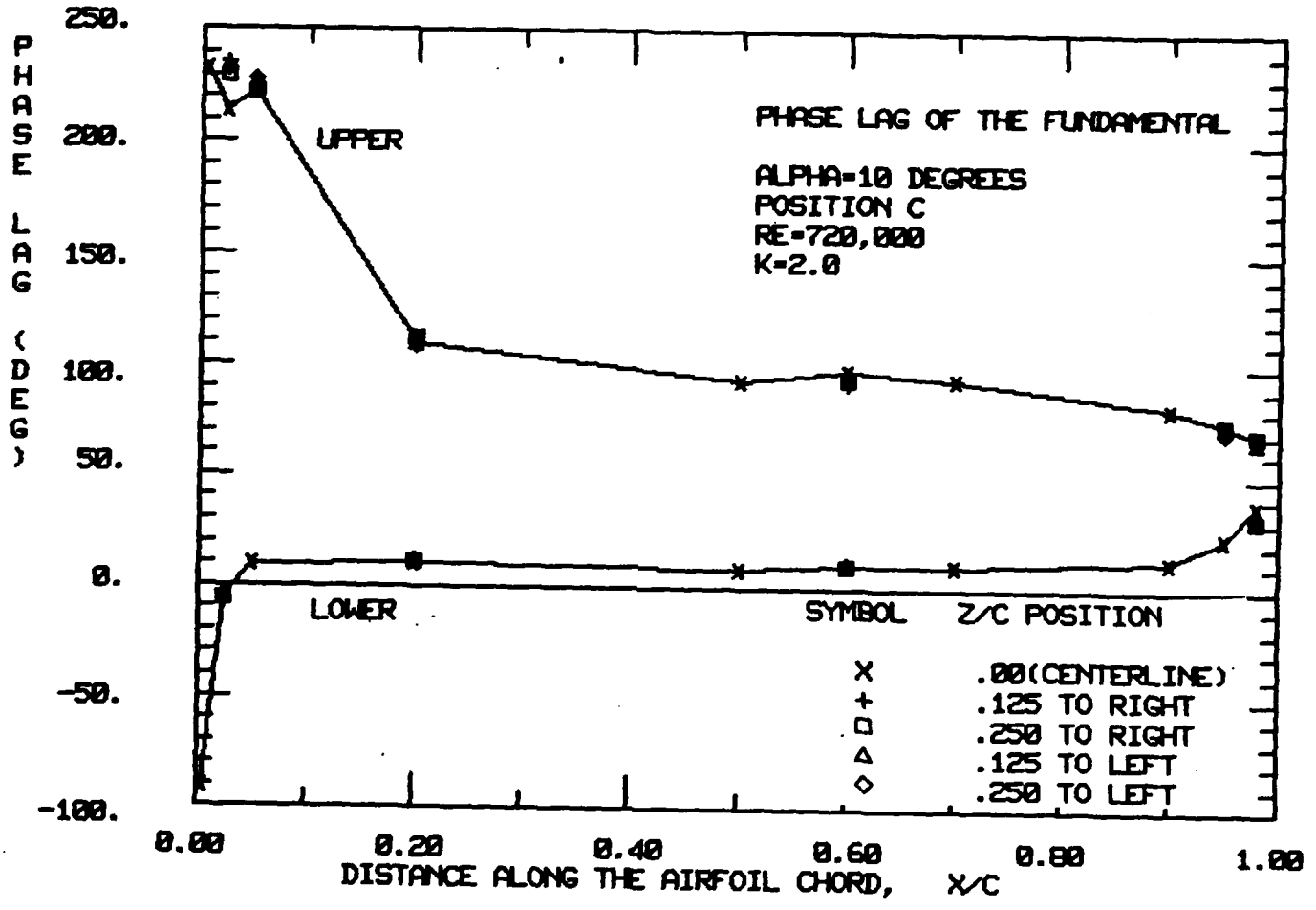

FIGURE 3C: SPANWISE DISTRIBUTION OF PHASE OF C_p - WITH LAMINAR SEPARATION BUBBLE

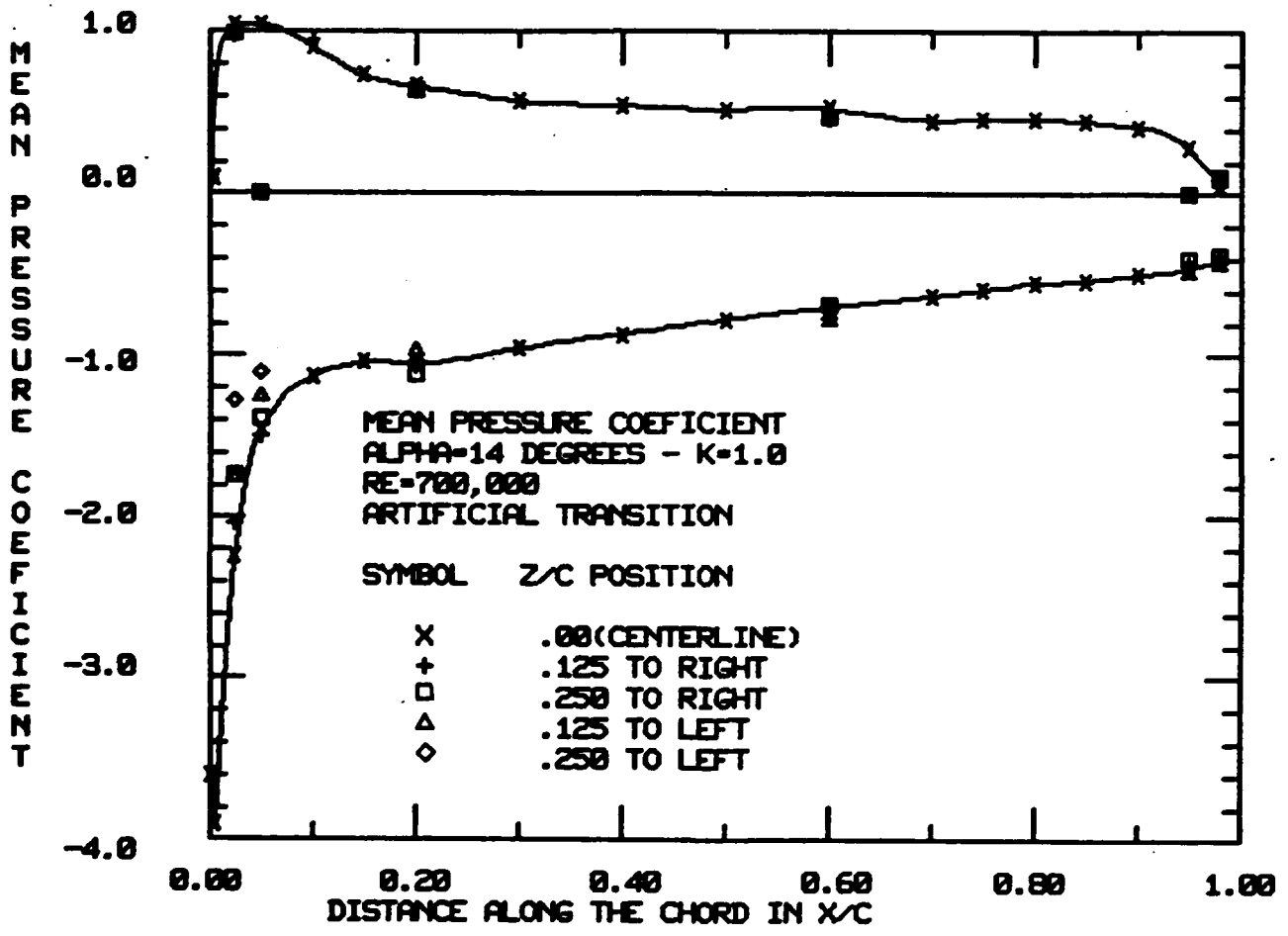

FIGURE 4A: SPANWISE DISTRIBUTION OF MEAN C_p WITH TURBULENT SEPARATION

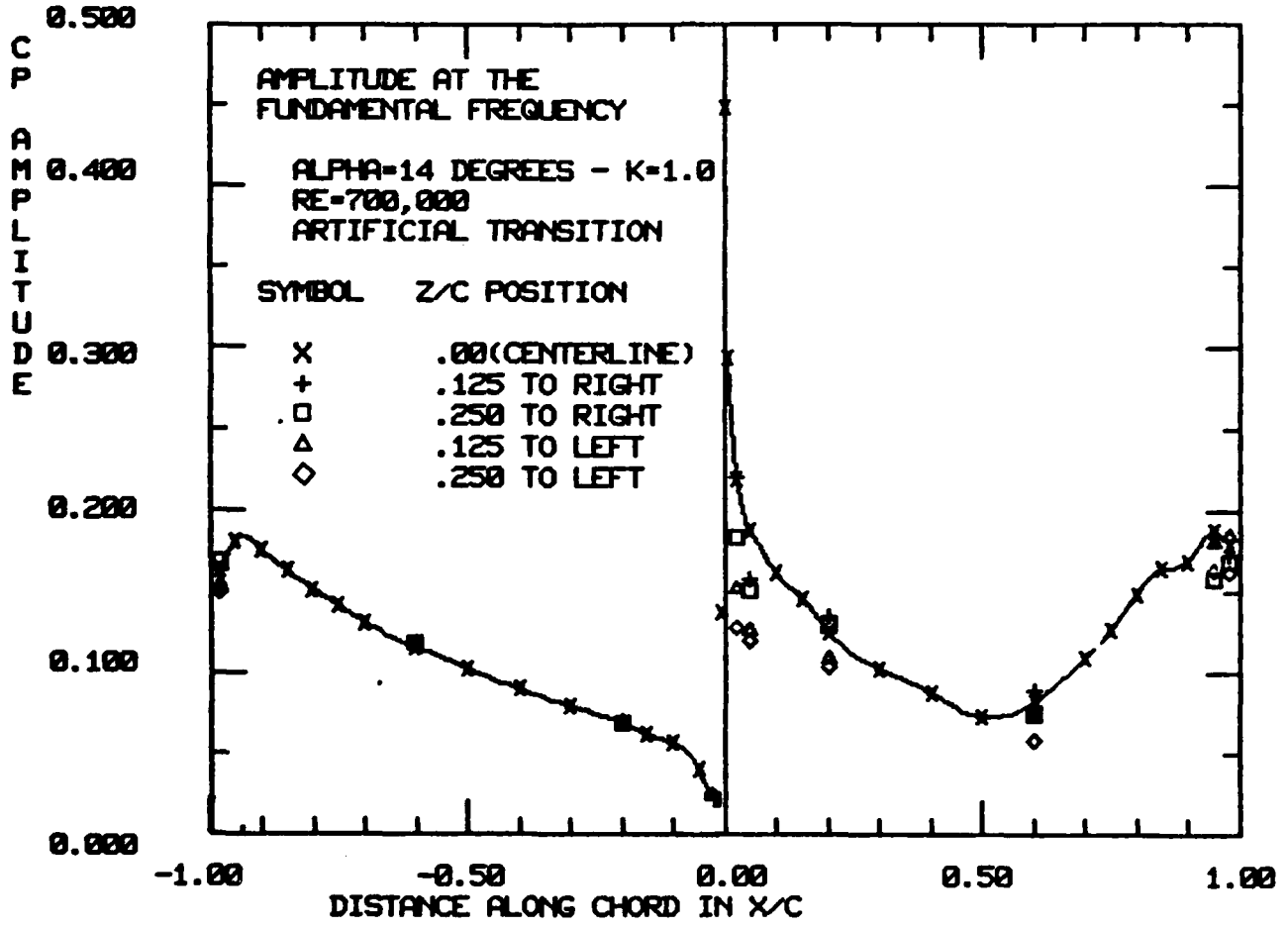

FIGURE 4B: SPANWISE DISTRIBUTION OF C_p WITH TURBULENT SEPARATION

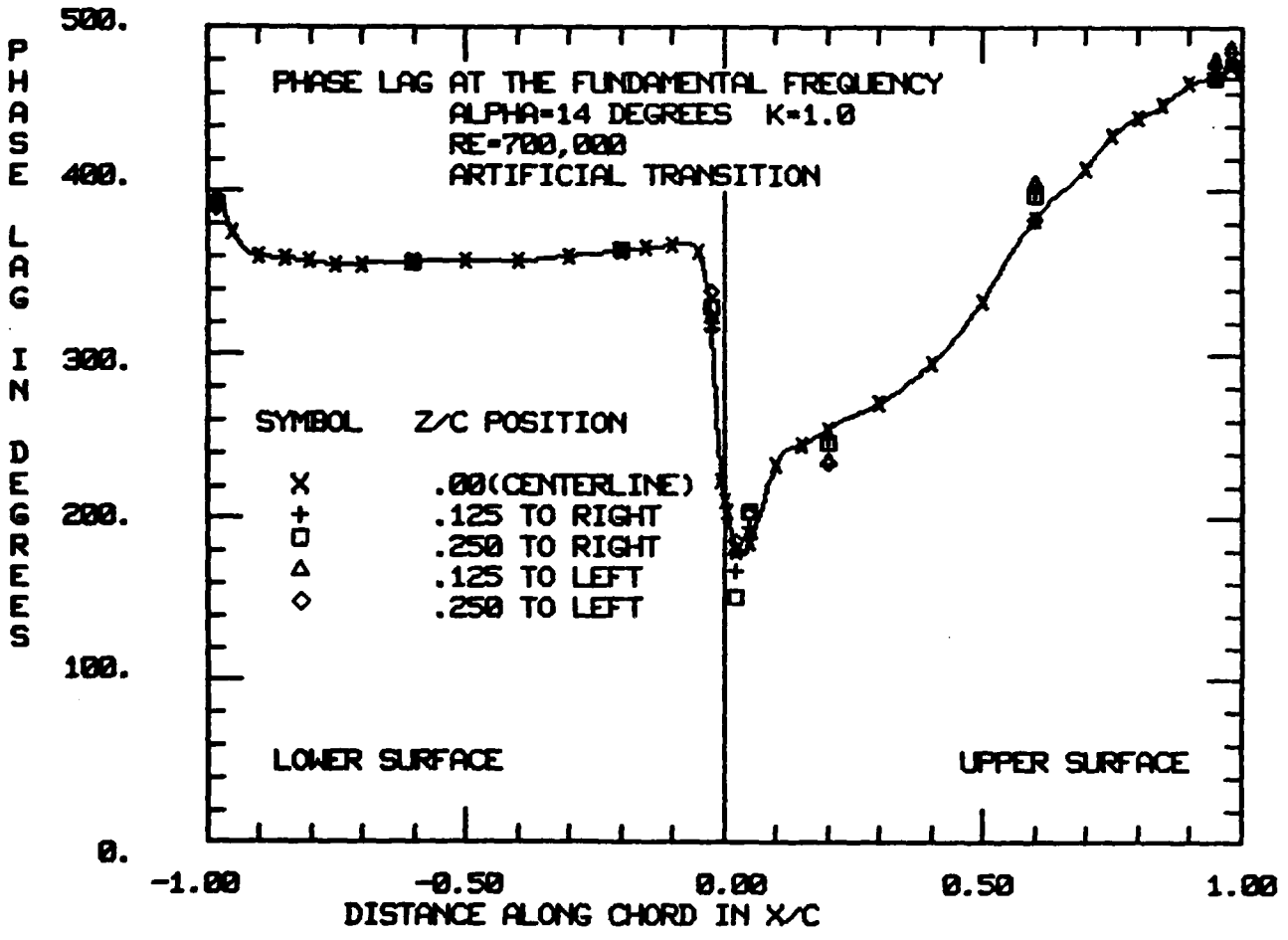

FIGURE 4C: SPANWISE DISTRIBUTION OF PHASE LAG OF C_p WITH TURBULENT SEPARATION

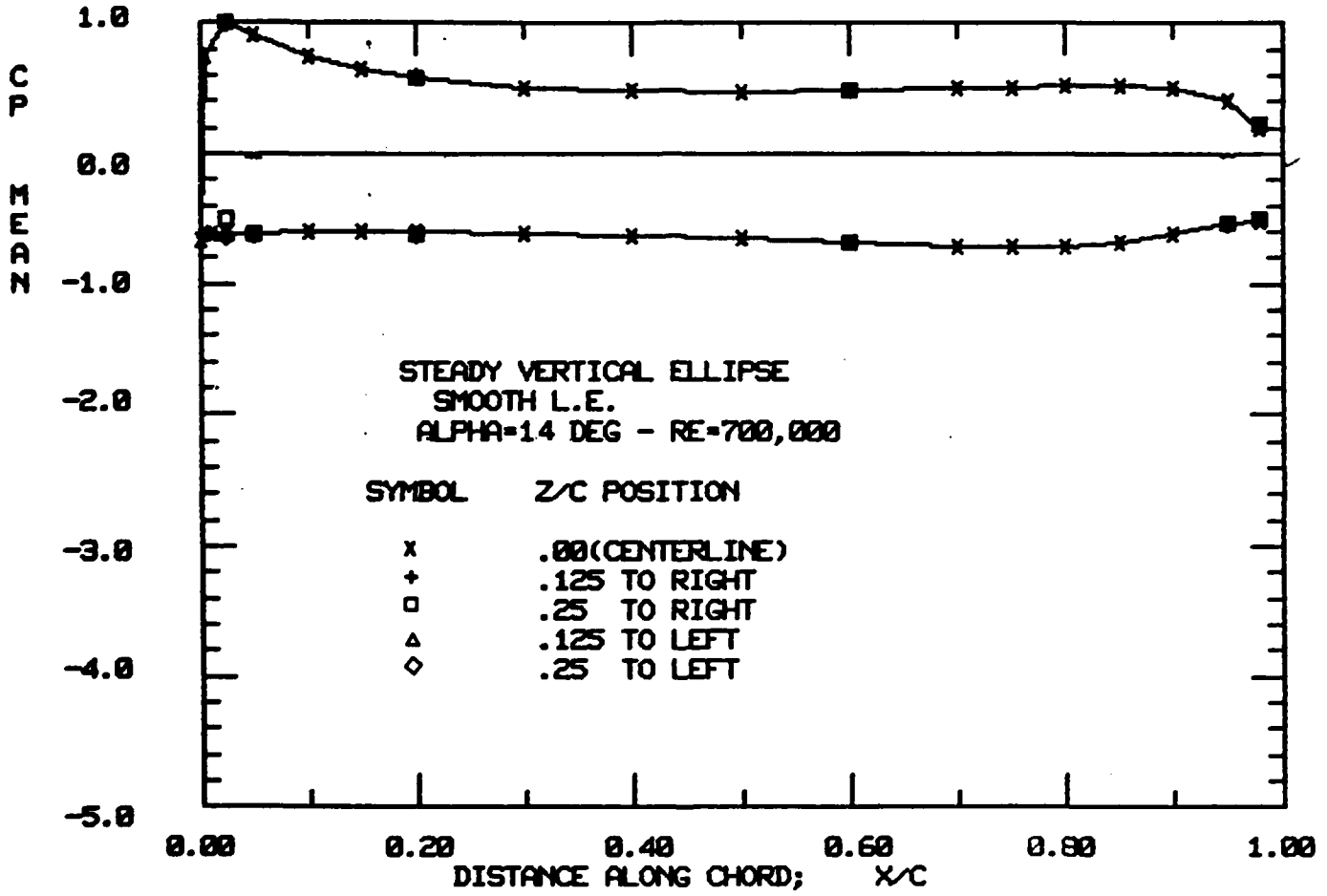

FIGURE 4D: SPANWISE DISTRIBUTION OF MEAN C_p FOR MASSIVE LAMINAR SEPARATION

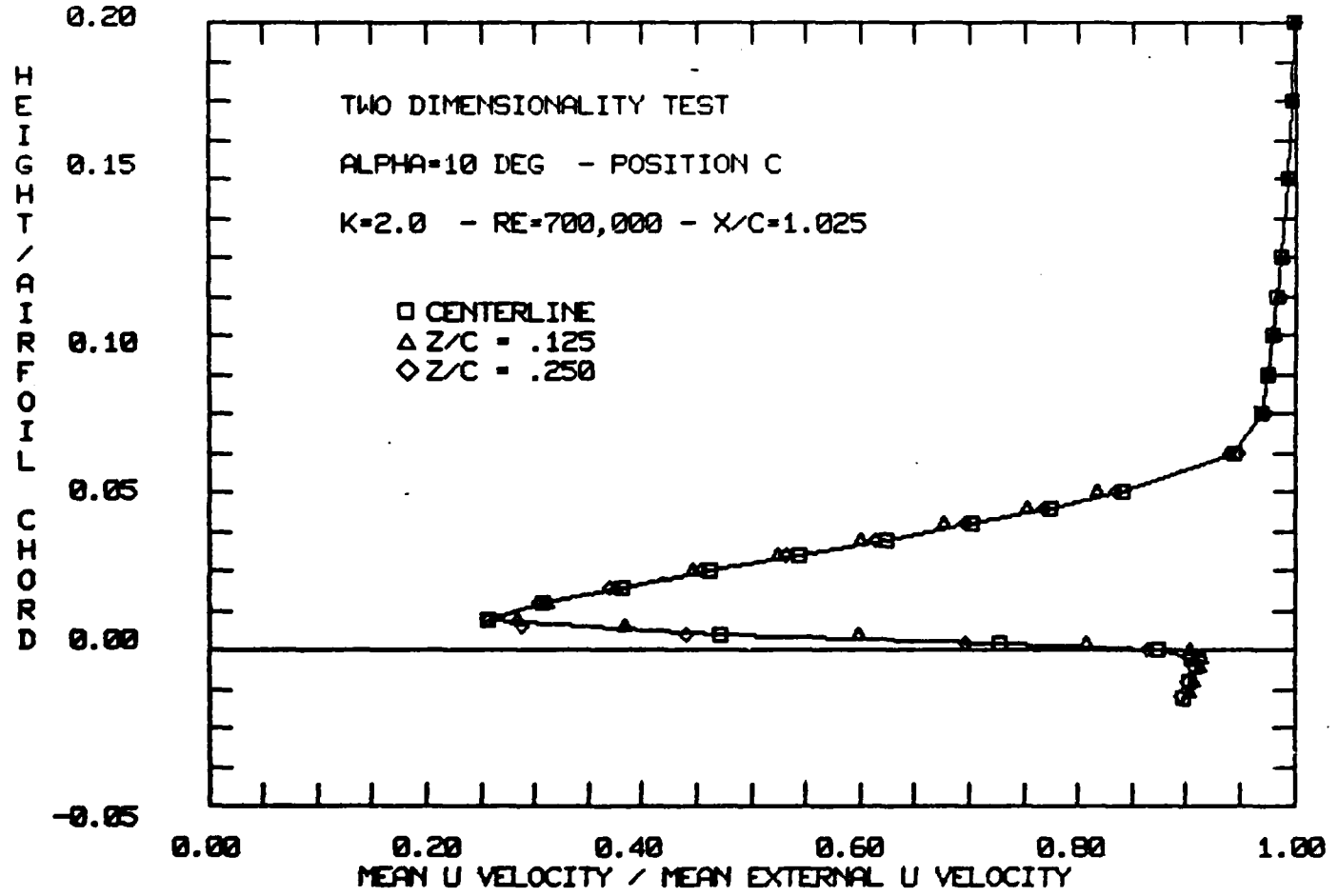

FIGURE 5A: SPANWISE DISTRIBUTION OF MEAN TANGENTIAL WAKE VELOCITY

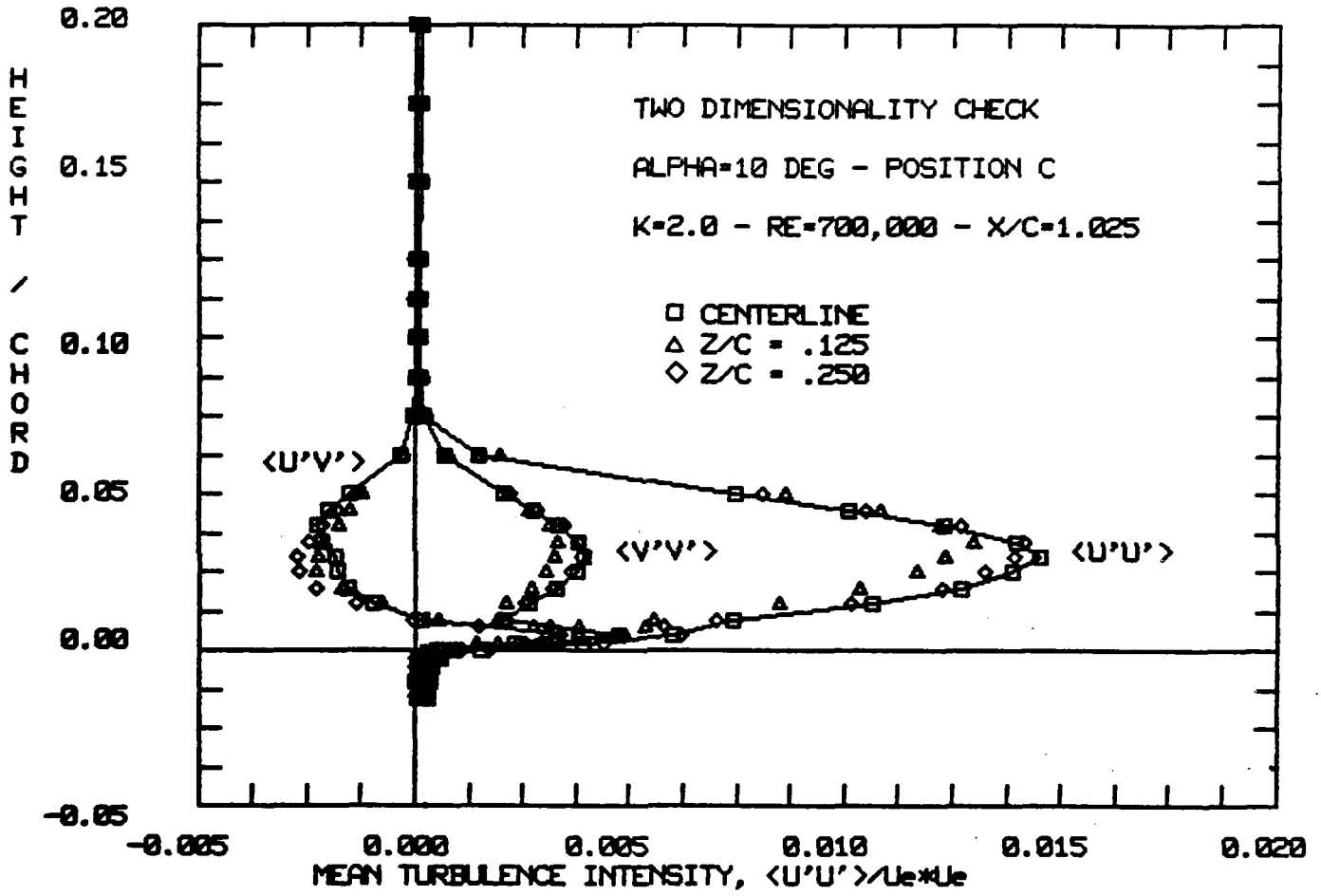

FIGURE 5B: SPANWISE DISTRIBUTION OF TURBULENT CHARACTERISTICS IN WAKE

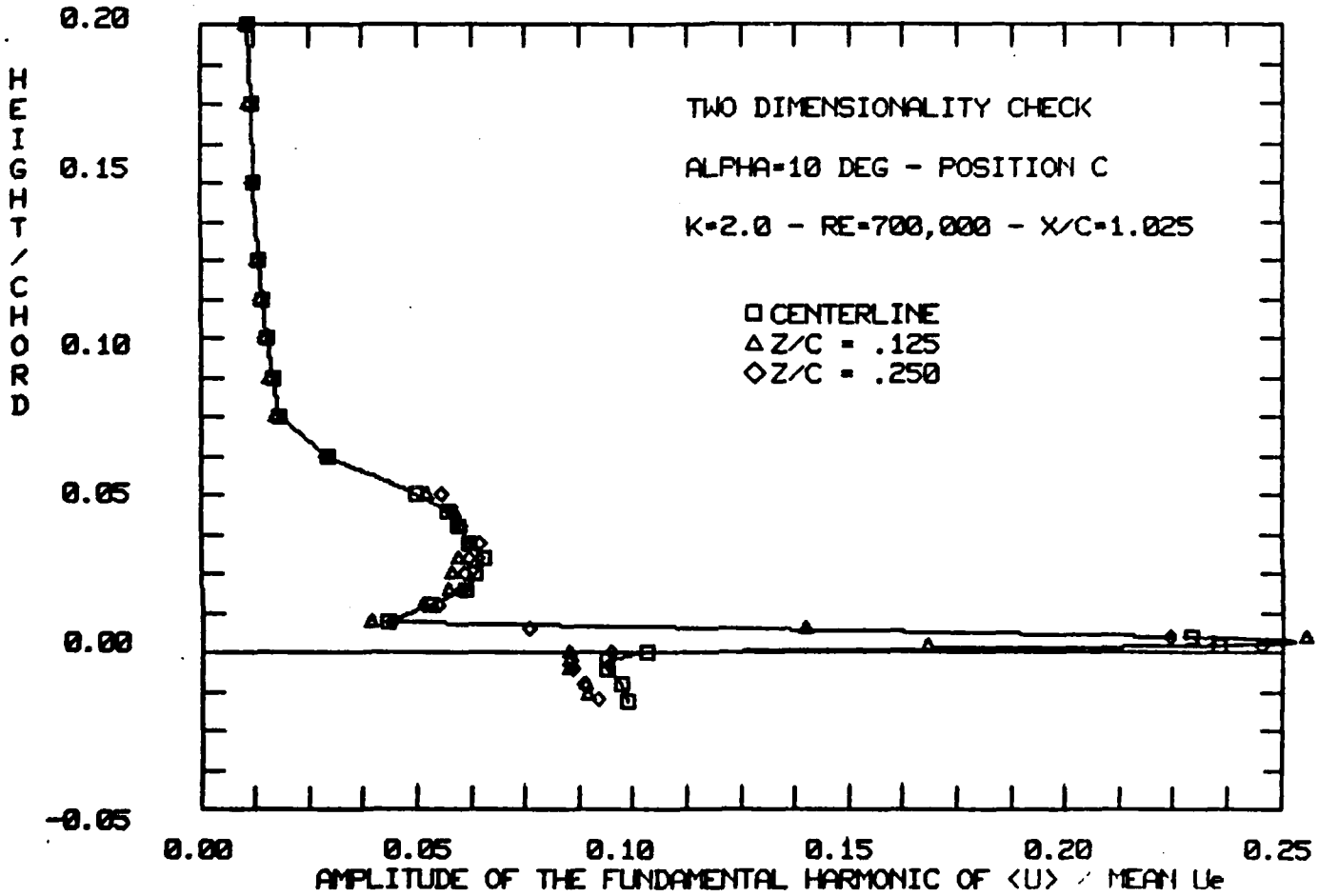

FIGURE 6A: SPANWISE DISTRIBUTION OF U IN WAKE

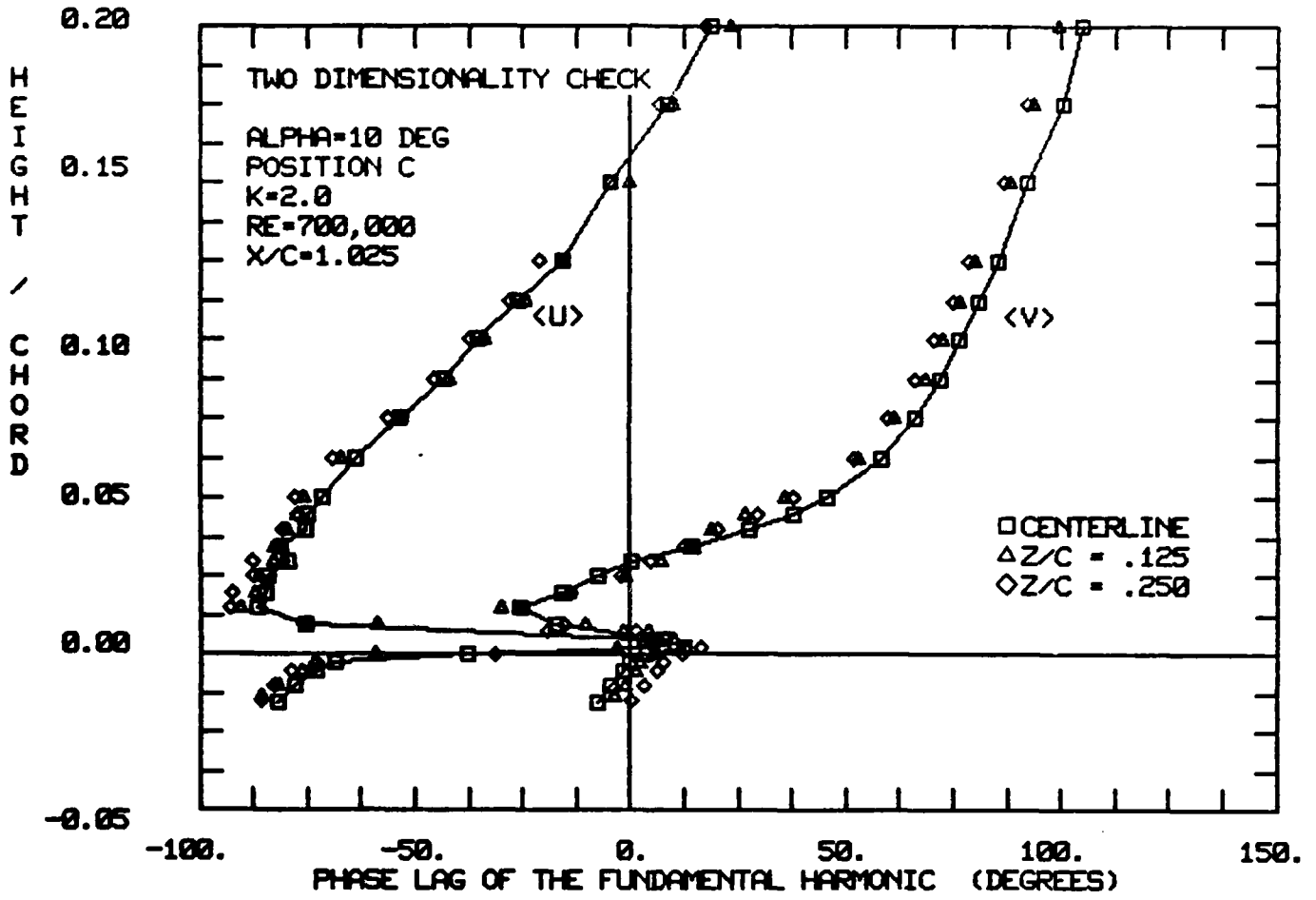

FIGURE 6B: SPANWISE DISTRIBUTION OF PHASE OF U AND V IN WAKE

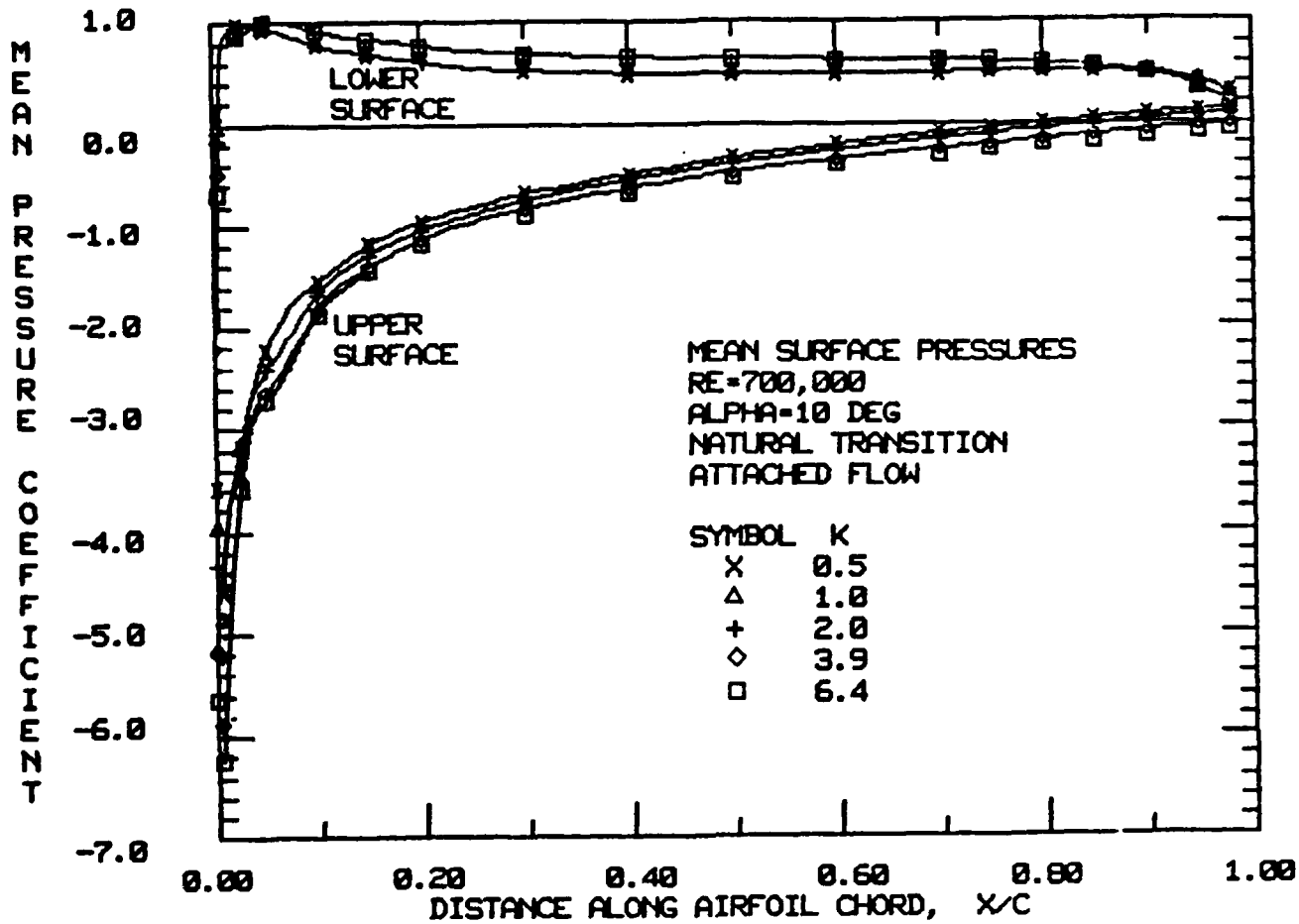

FIGURE 7: EFFECT OF "k" UPON $\overline{C_p}$ DISTRIBUTION IN ATTACHED FLOW

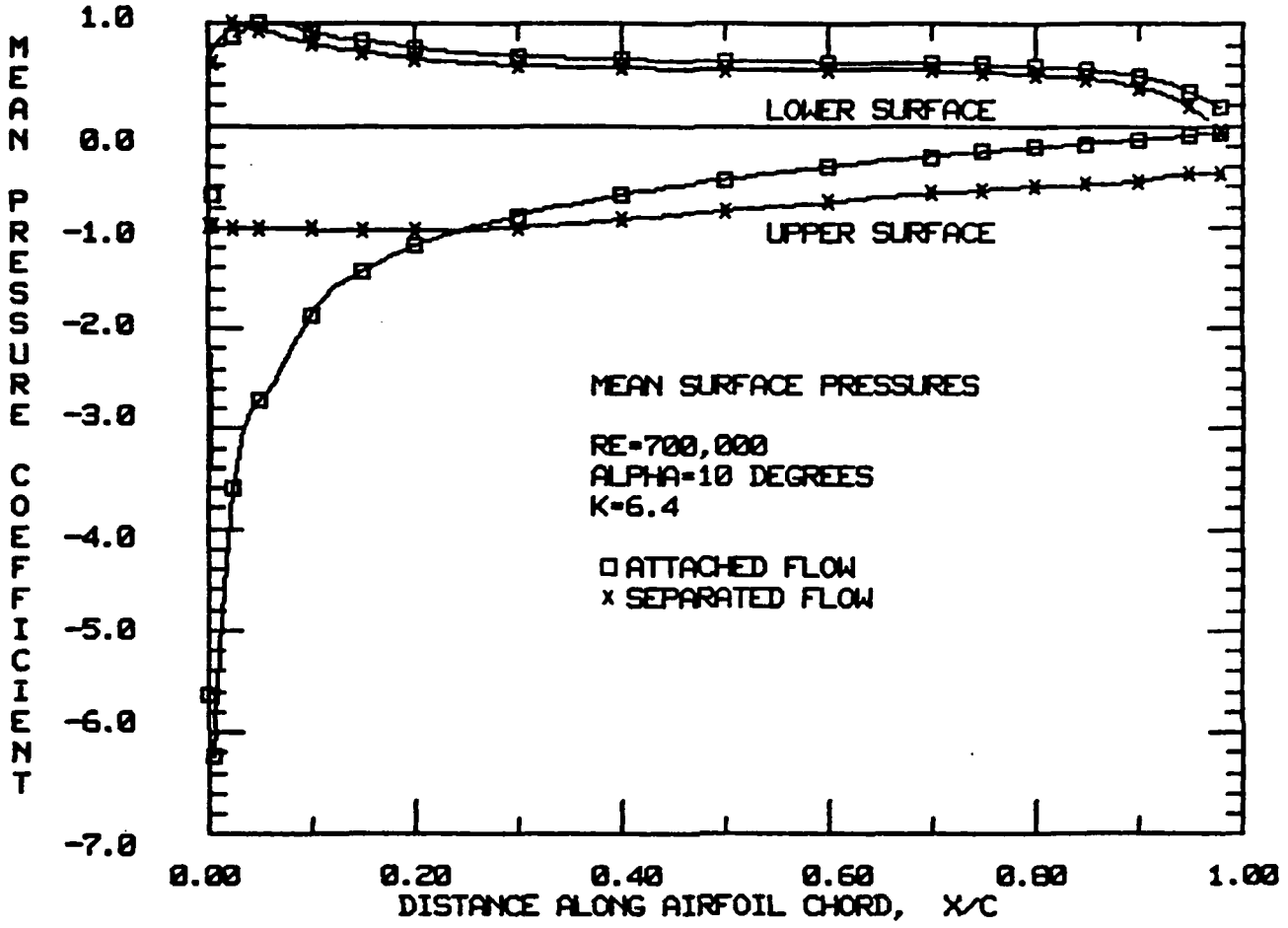

FIGURE 8: EFFECT OF SEPARATION ON $\overline{C_p}$ AT K=6.4

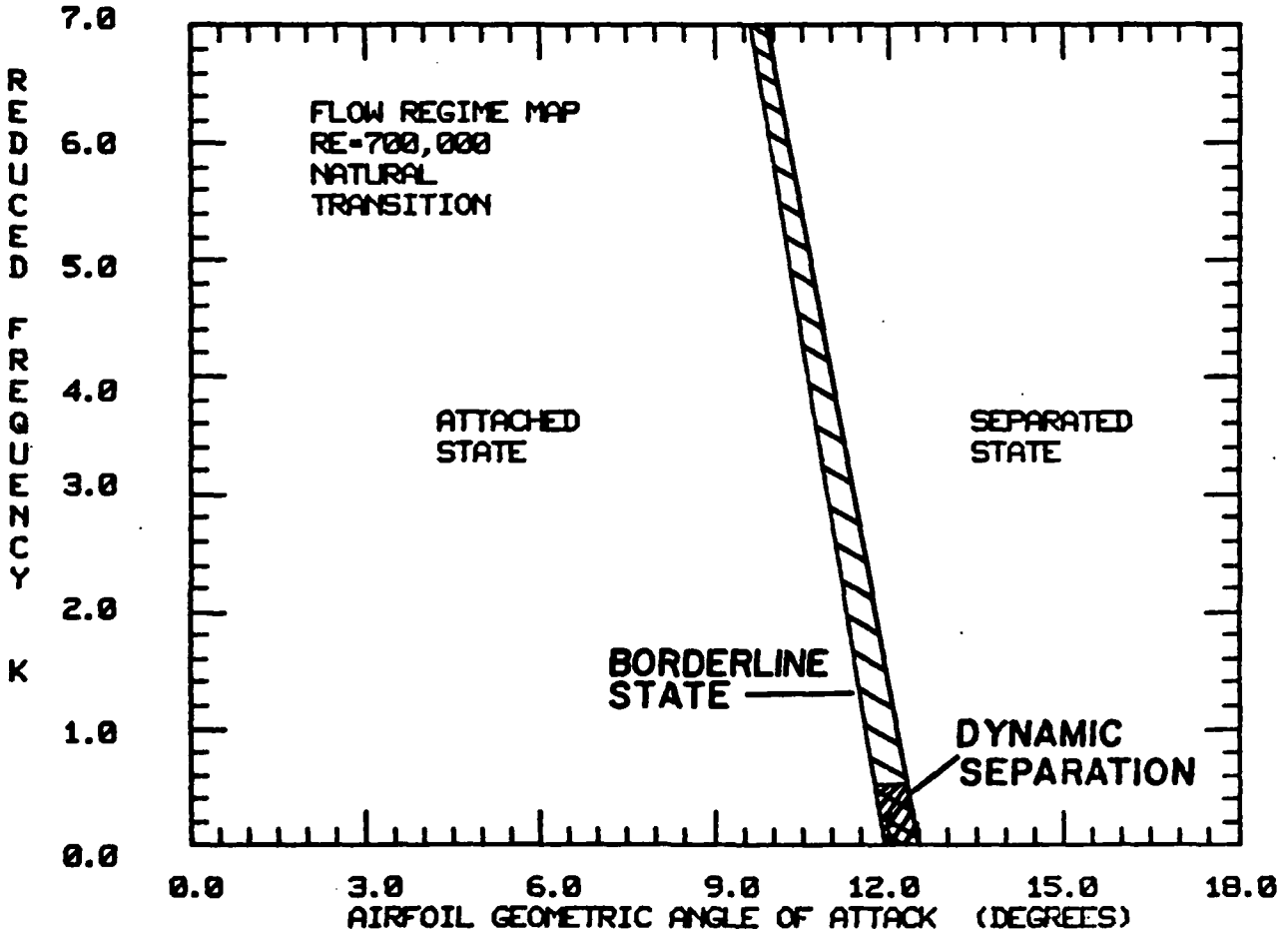

FIGURE 9: CHARACTERISTIC STATE WITH NATURAL TRANSITION (R_e=700,000)

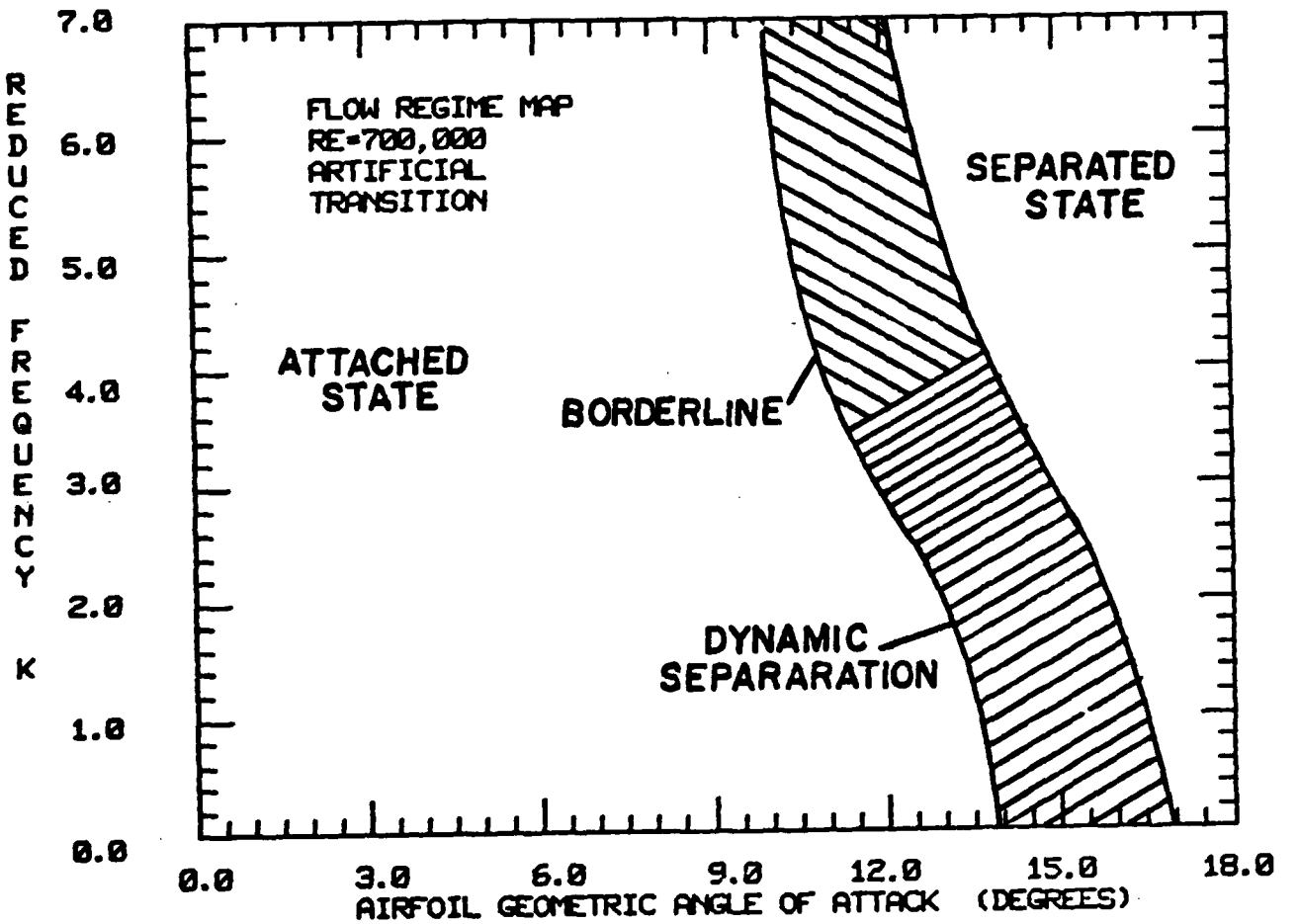

FIGURE 10: CHARACTERISTIC STATE
ARTIFICIAL TRANSITION

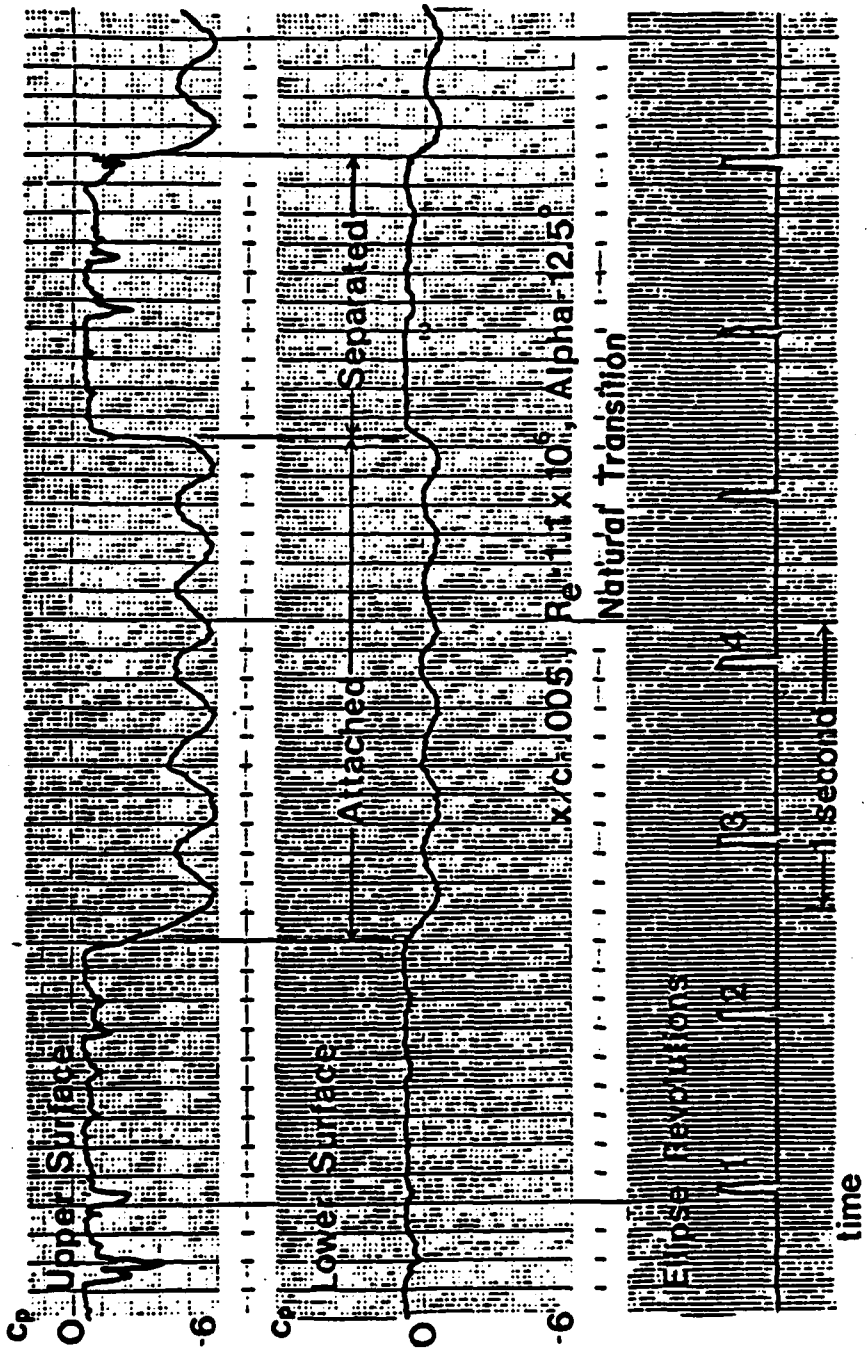

FIGURE 11: TIME RESOLVED MEASUREMENT OF "DYNAMIC SEPARATION"

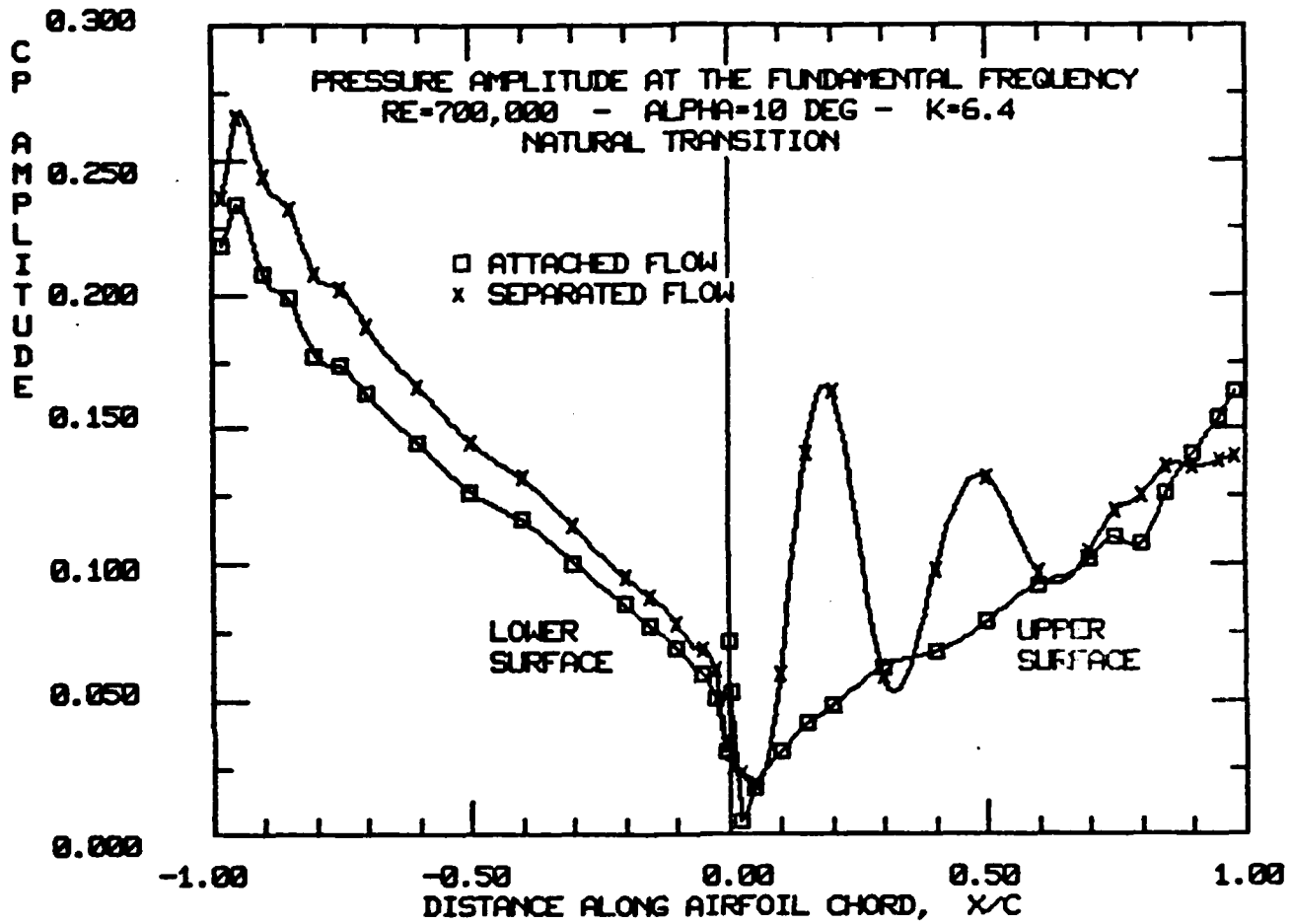

FIGURE 12: AMPLITUDE OF C_p AS A FUNCTION OF X/C FOR K=6.4

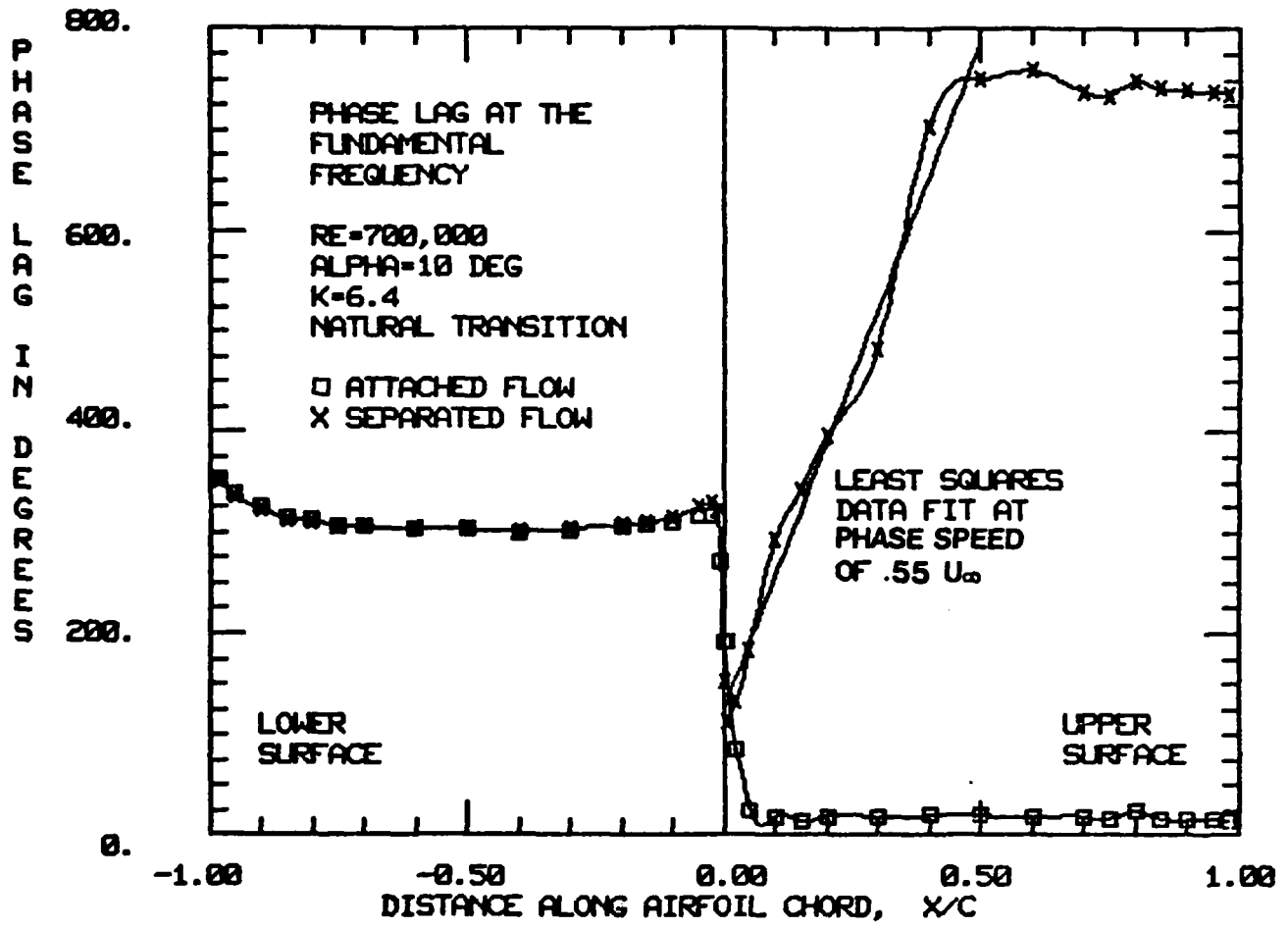

FIGURE 13: DISTRIBUTION OF PHASE OF C_p AT K=6.4

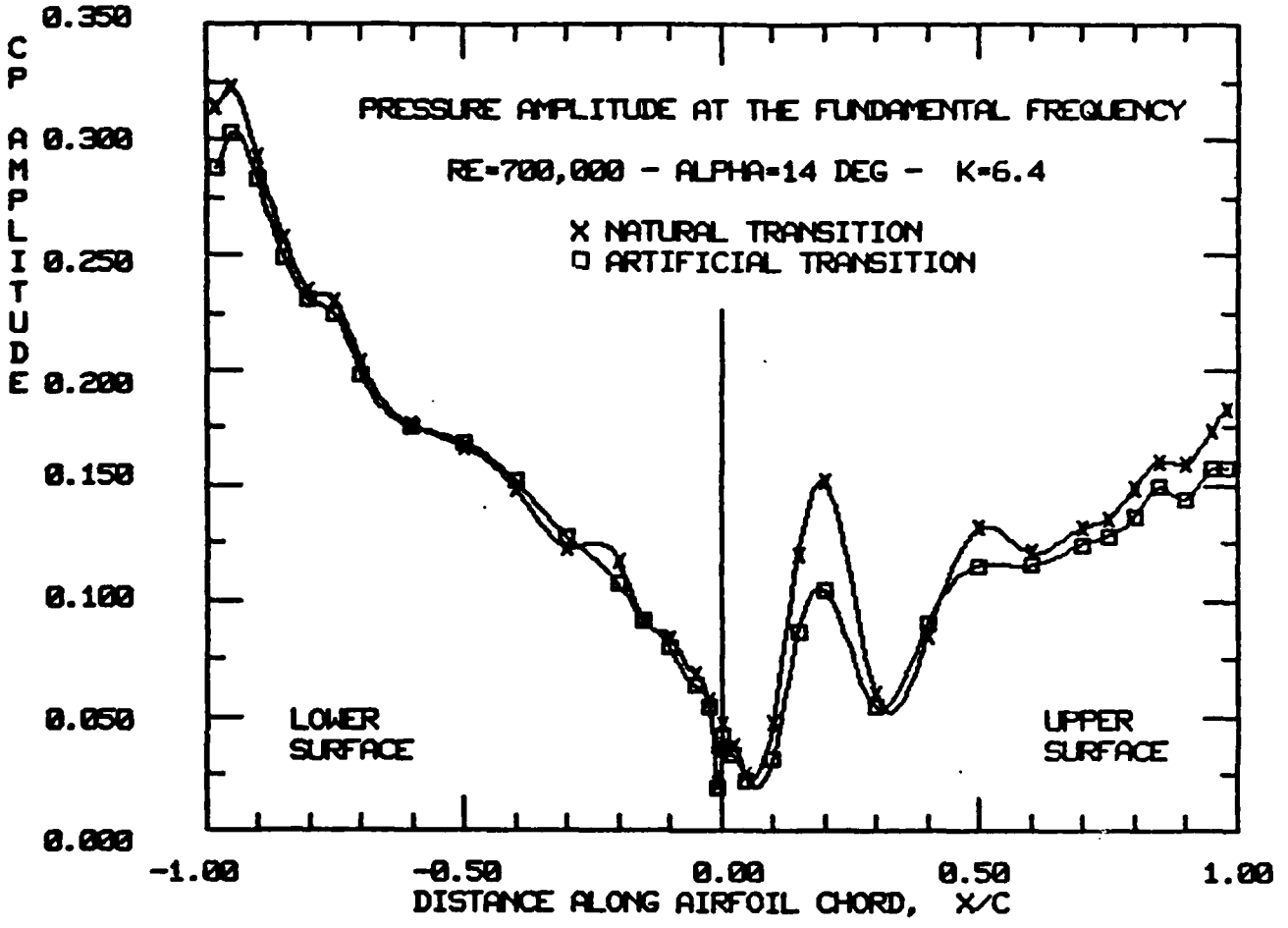

FIGURE 14: EFFECT OF TRANSITION ON AMPLITUDE OF C_p

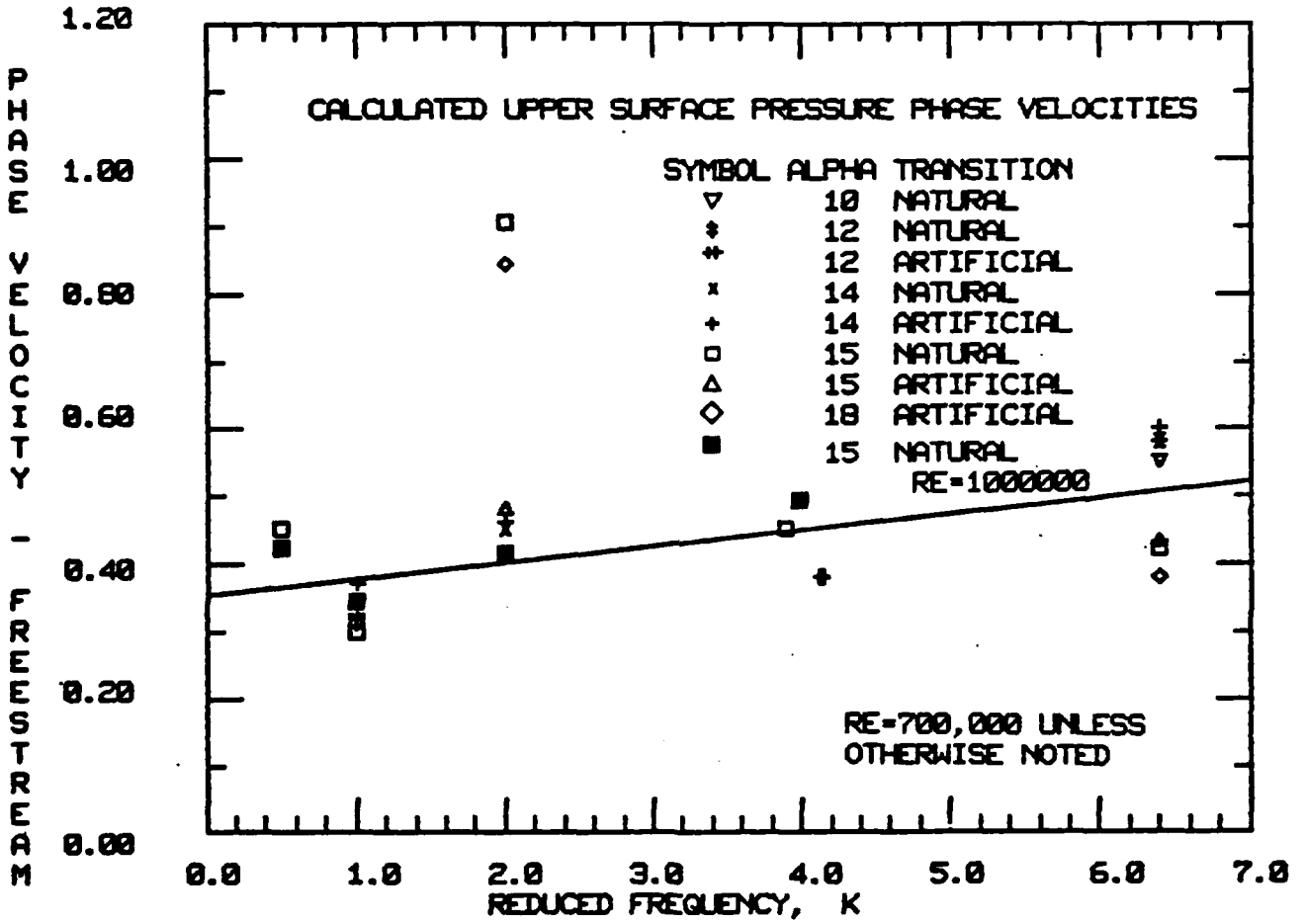

FIGURE 15: PHASE VELOCITY AS A FUNCTION OF "K"

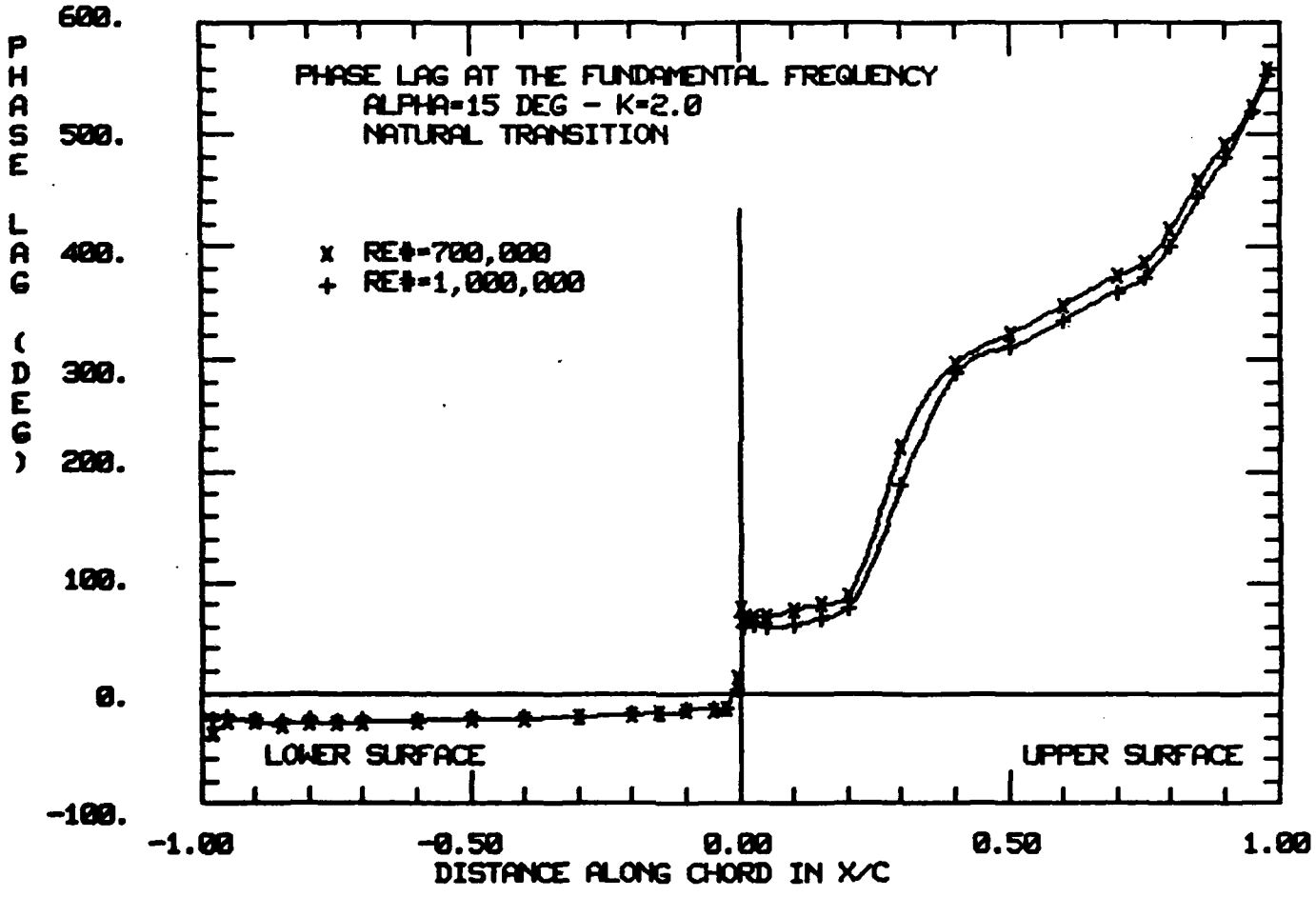

FIGURE 16A: EFFECT OF REYNOLDS NUMBER ON PHASE OF C_p

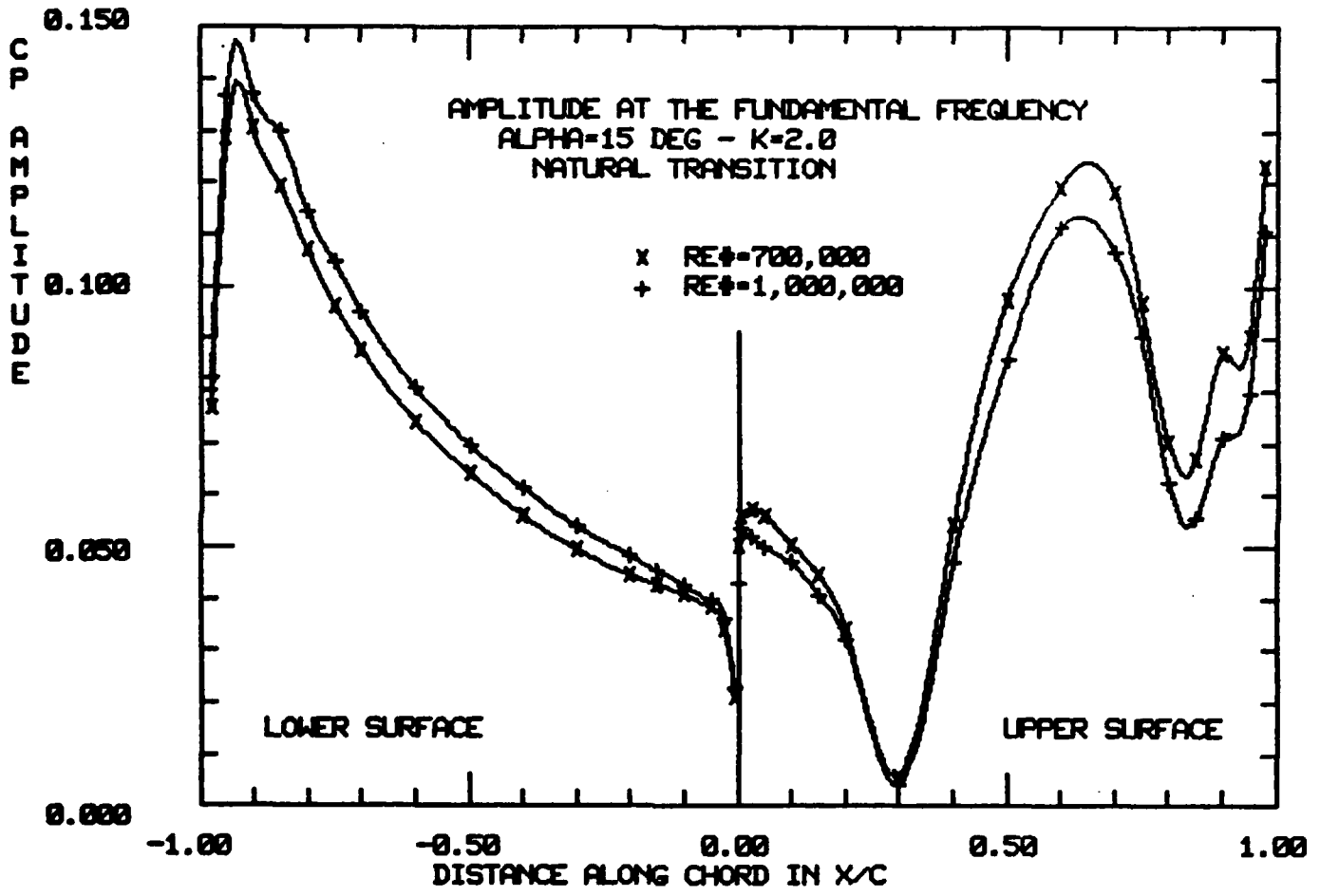

FIGURE 16B: EFFECT OF REYNOLDS NUMBER ON AMPLITUDE OF C_p

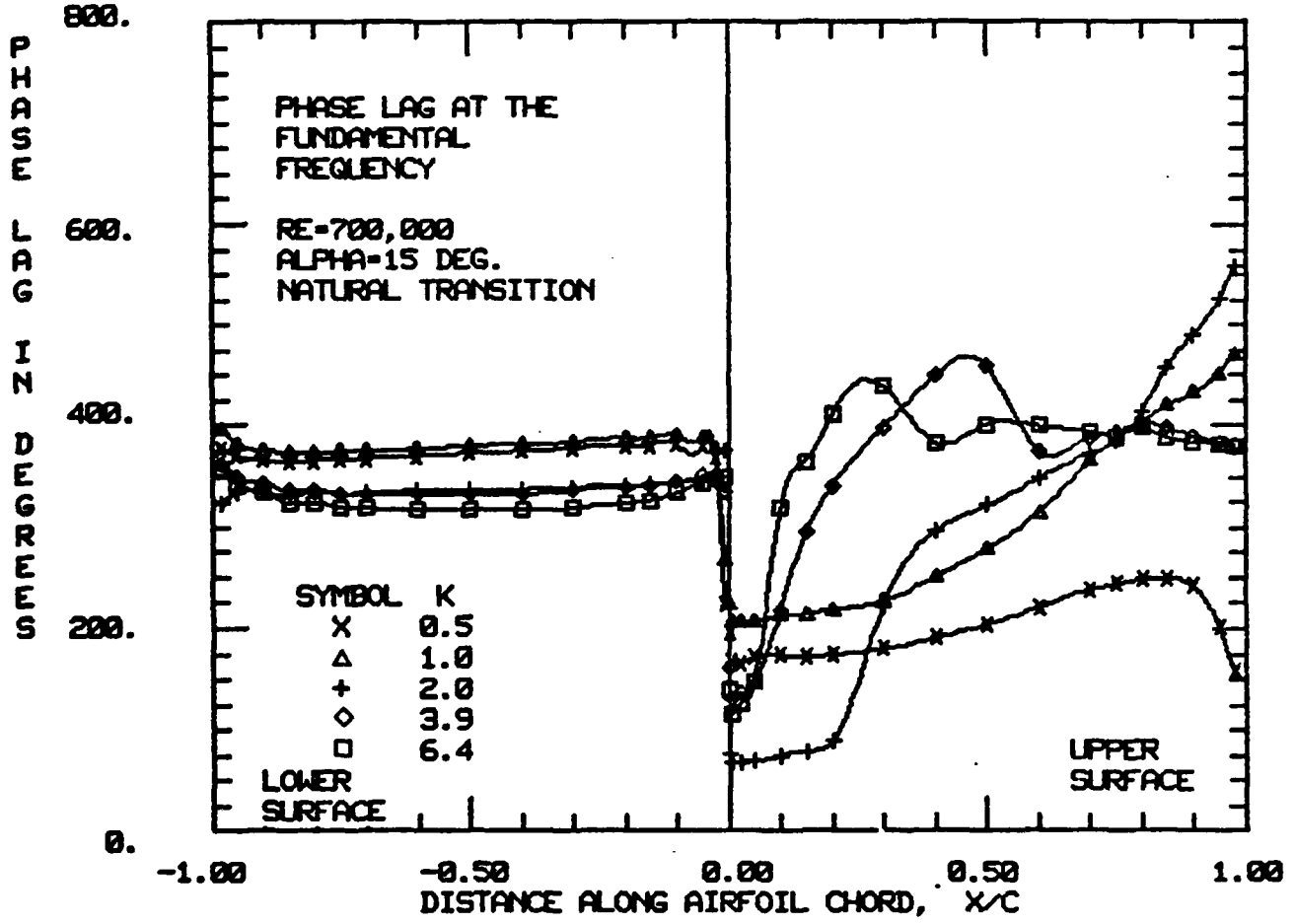

FIGURE 17A: EFFECT OF K ON PHASE LAG OF C_p

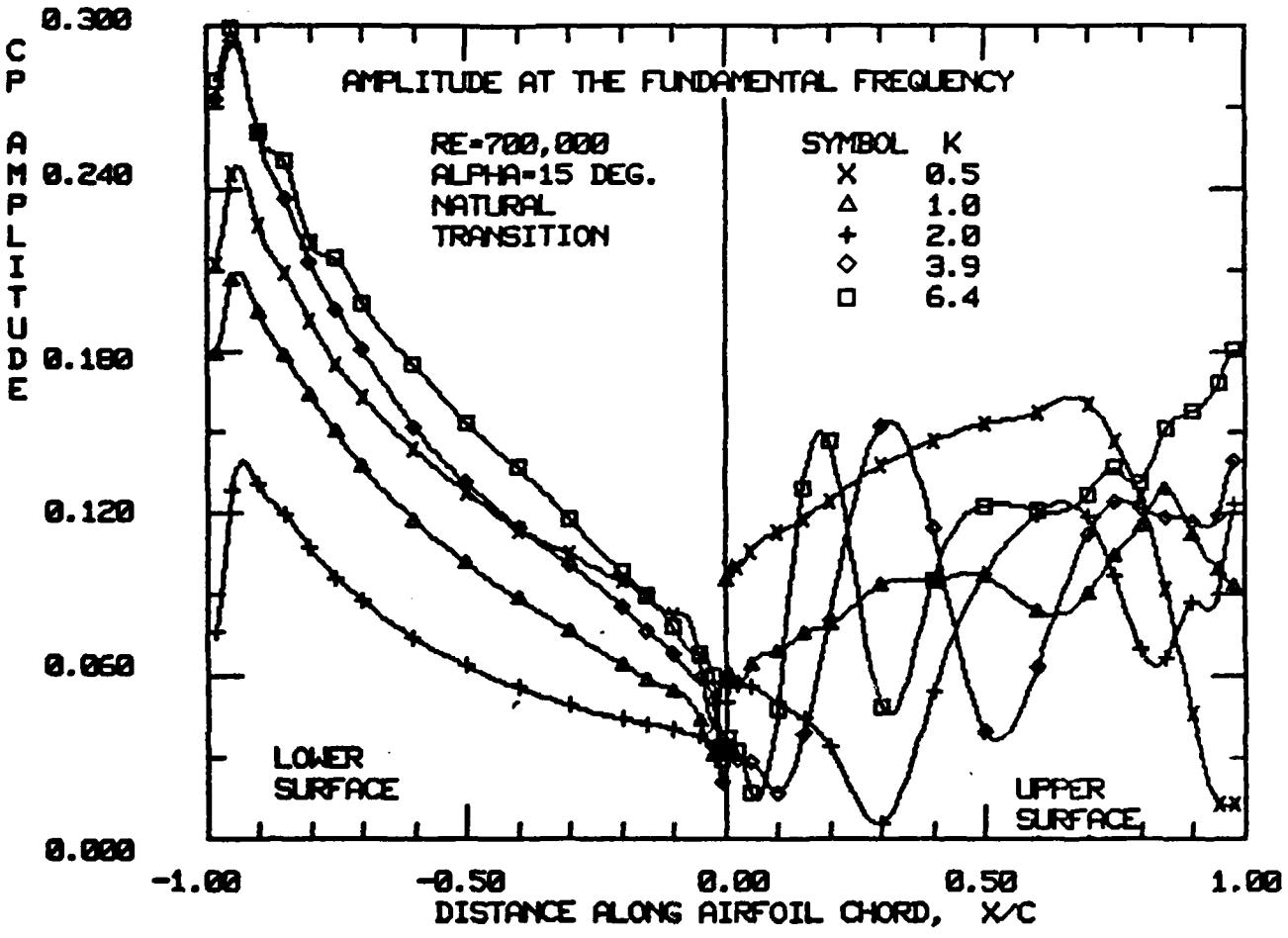

FIGURE 17B: EFFECT OF K ON AMPLITUDE OF C_p

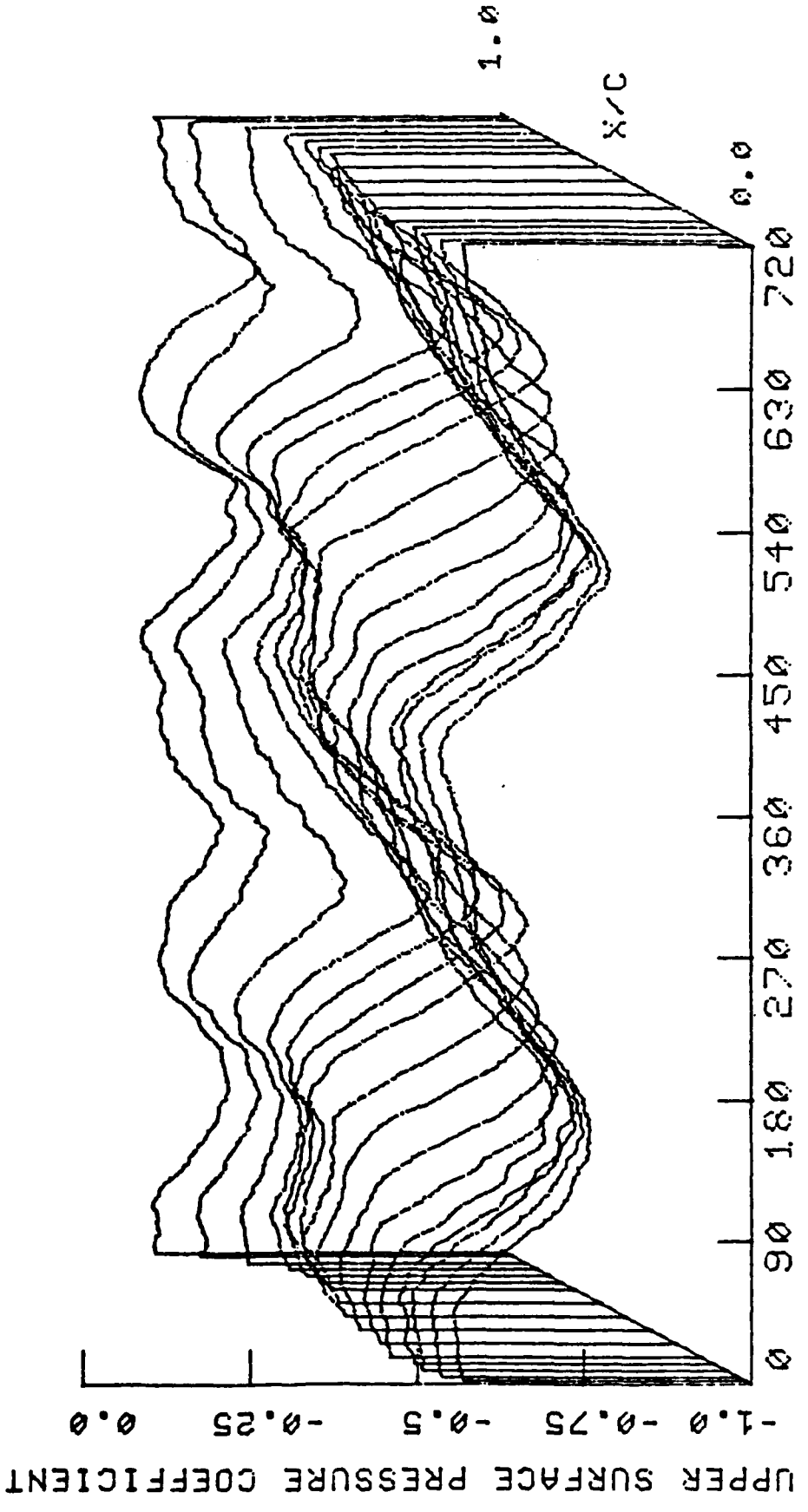

FIGURE 18: EXAMPLE OF FREQUENCY DOUBLING AT TRAILING EDGE

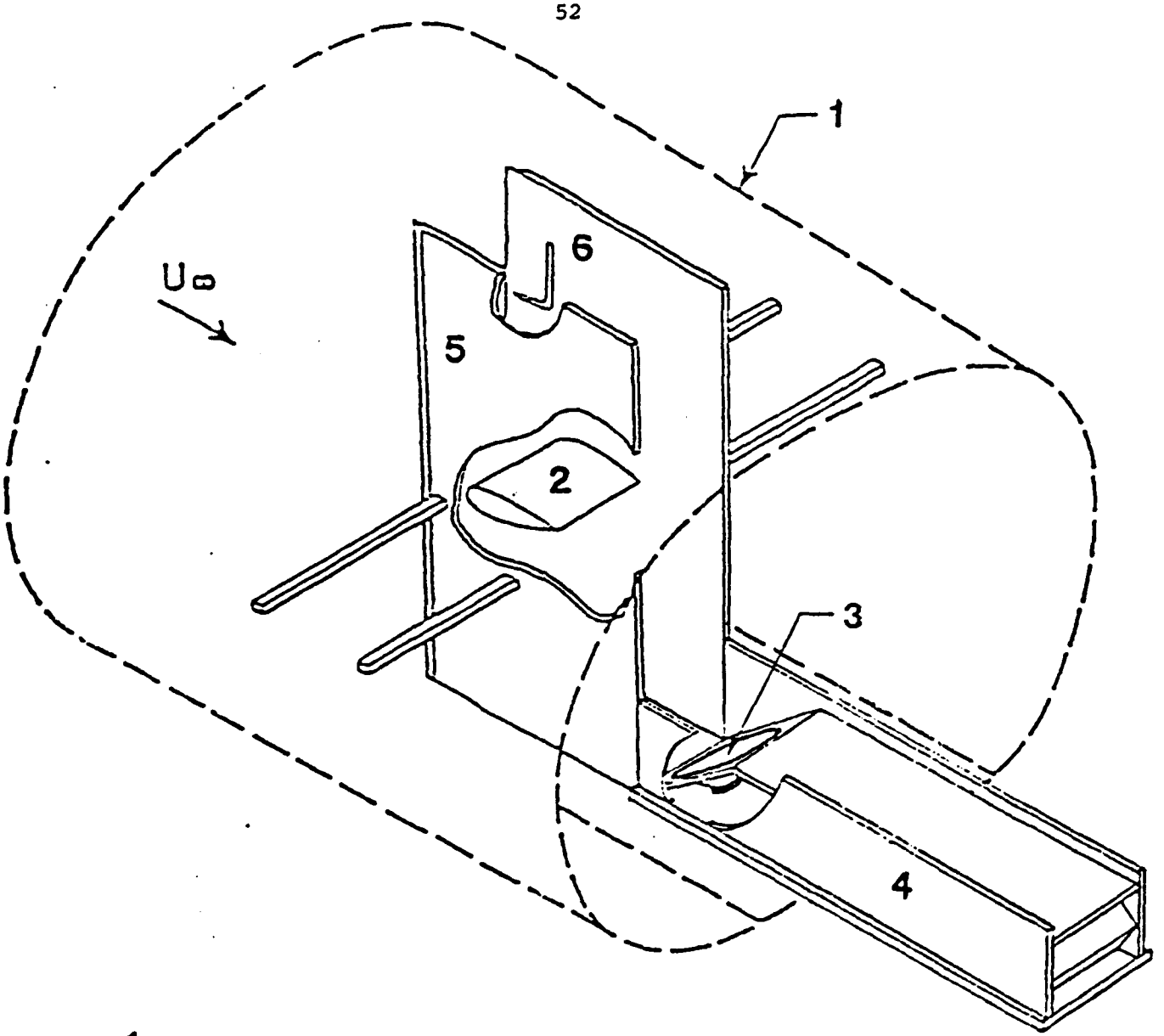

1 - TEST SECTION
2 - AIRFOIL
3 - LOUDSPEAKER
4 - ENCLOSURE
5 - SIDEBOARD
6 - PITOT PROBE

FIGURE 19: GENERAL ARRANGEMENT OF ACOUSTIC EXPERIMENT

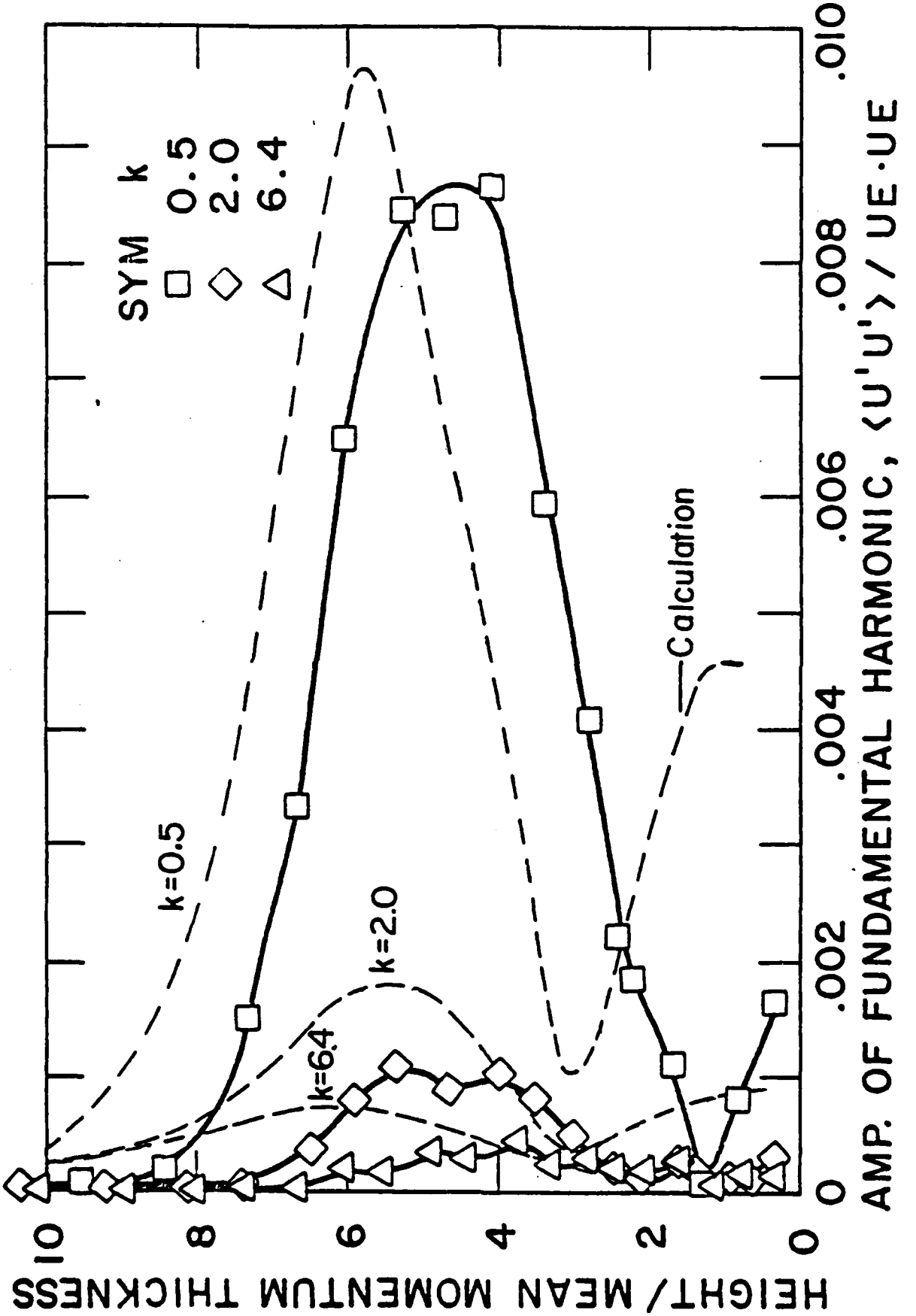

FIGURE 20: CALCULATED AND MEASURED VALUE OF $U'U'/V_E^2$ BASED UPON GEOMETRIC ARGUMENT

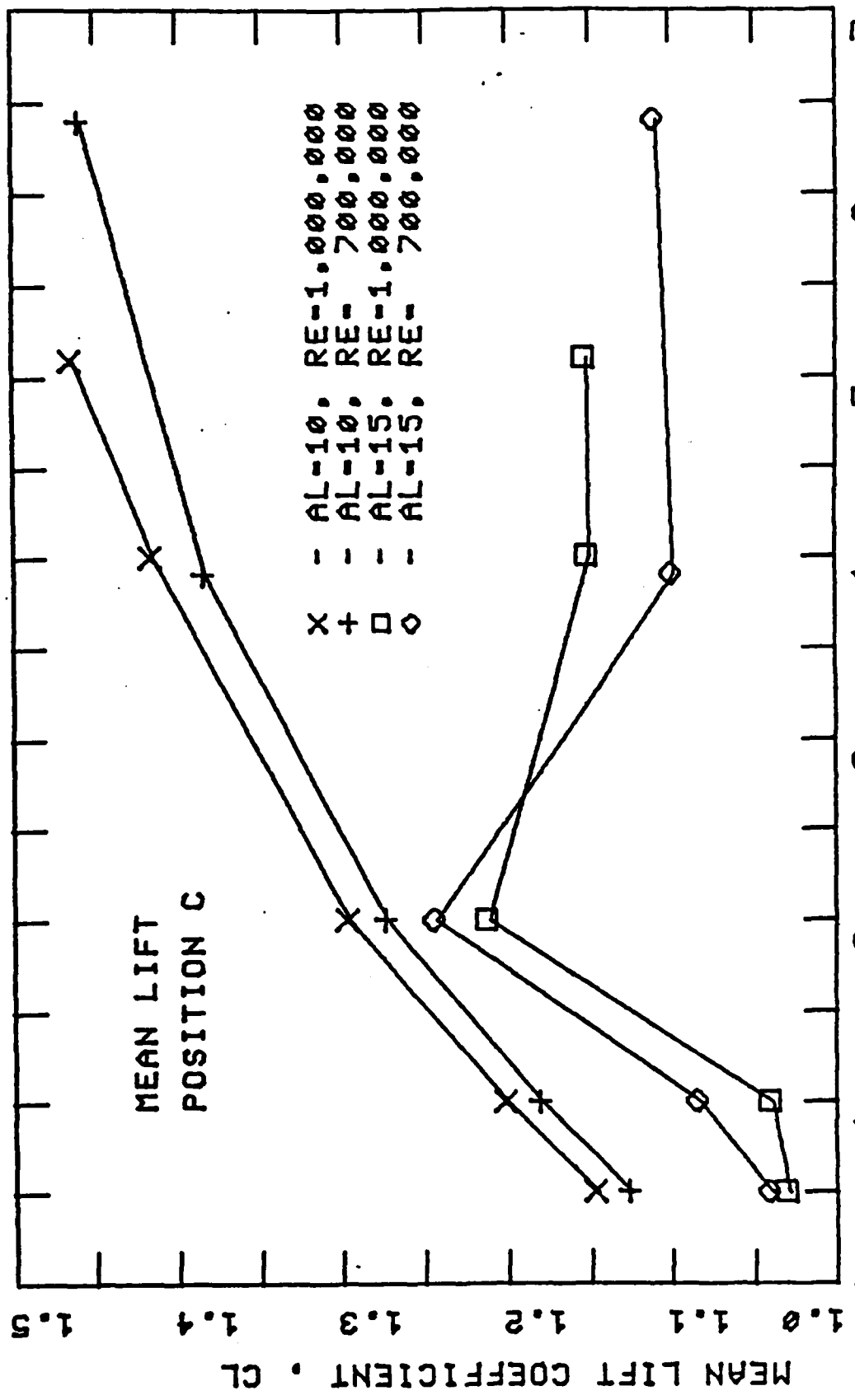

FIGURE 21: $\overline{C_L}$ AS A FUNCTION OF K

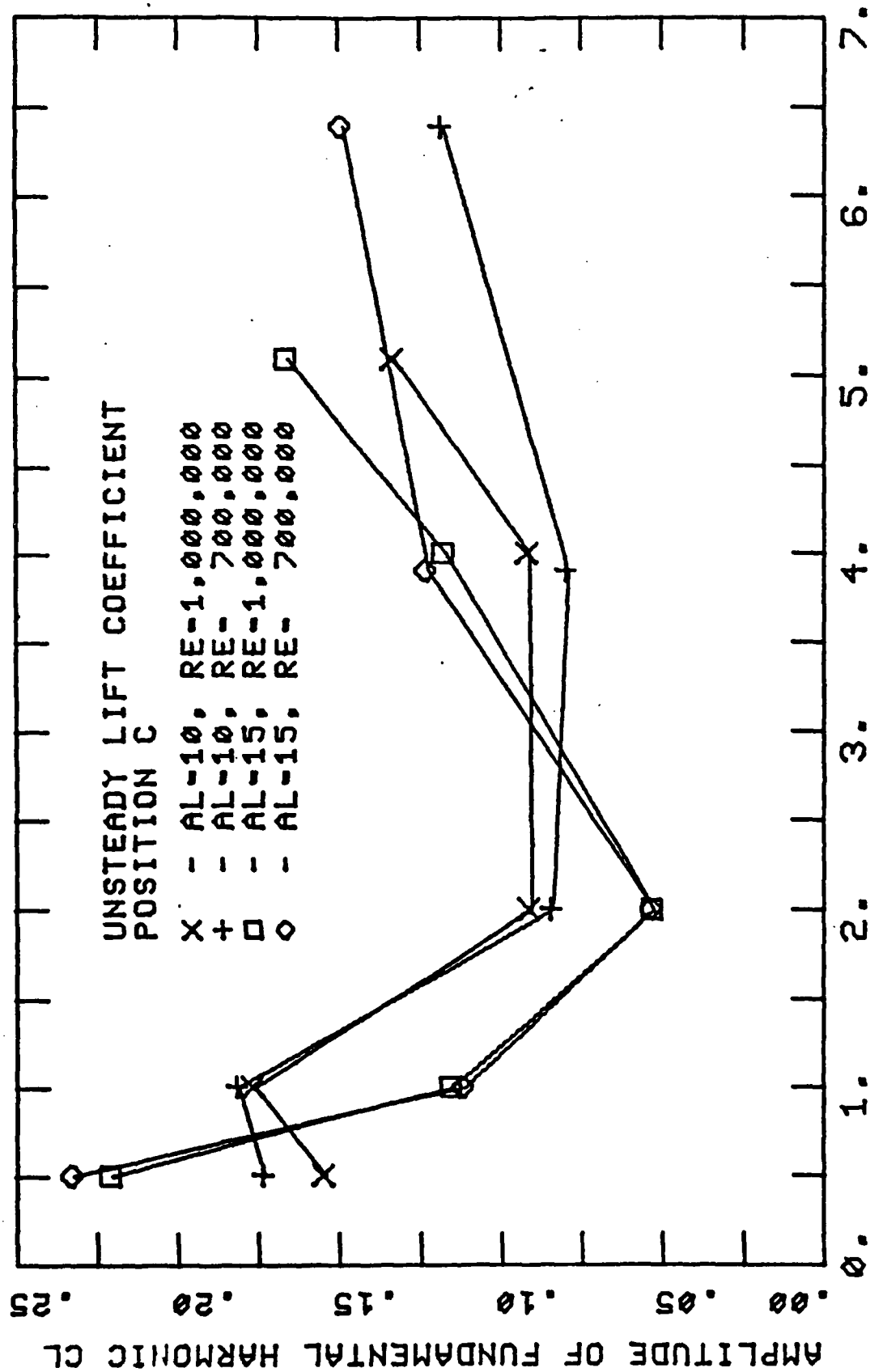

FIGURE 22: AMPLITUDE OF C_L AS A FUNCTION OF K

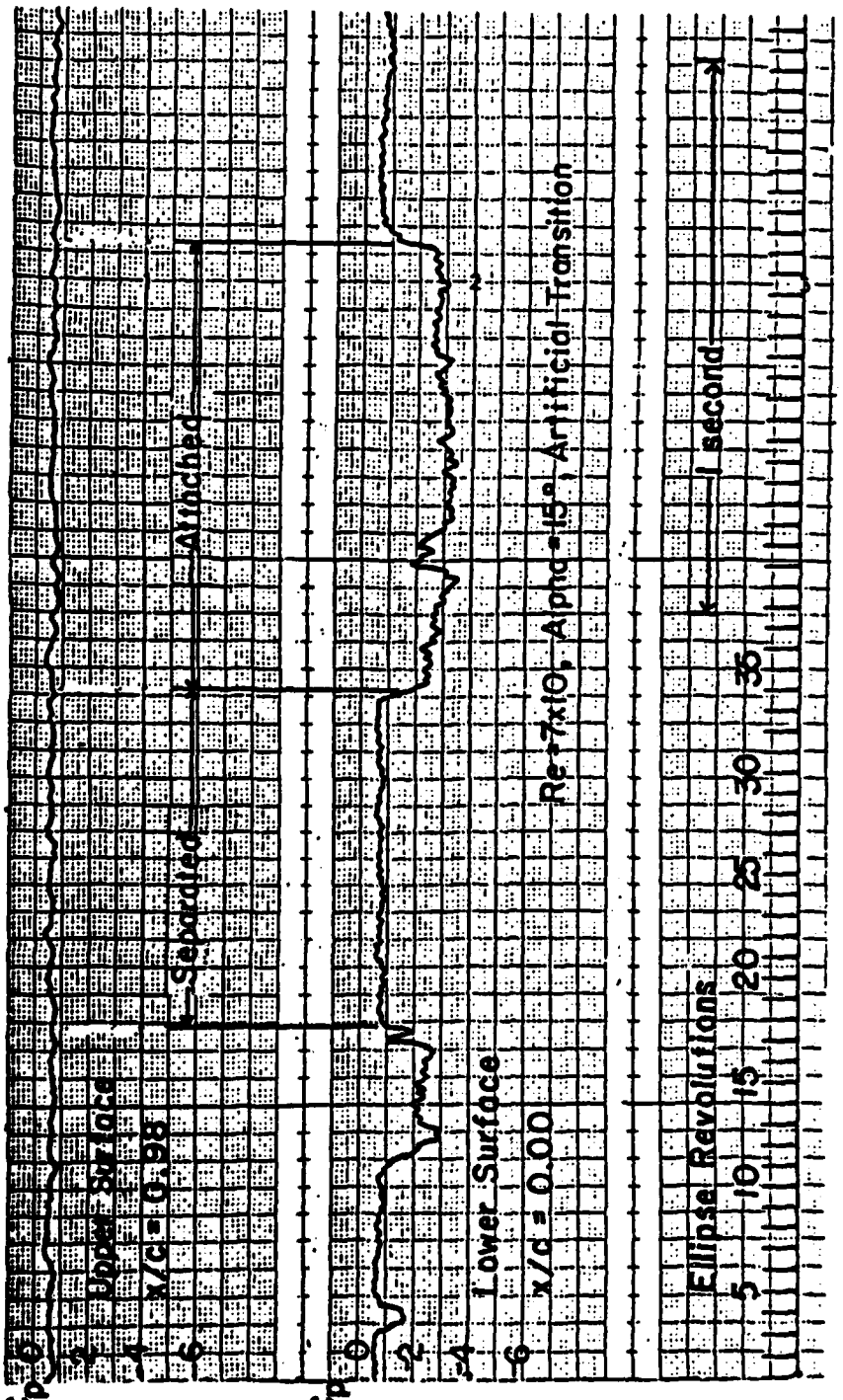

FIGURE 23: DYNAMIC SEPARATION

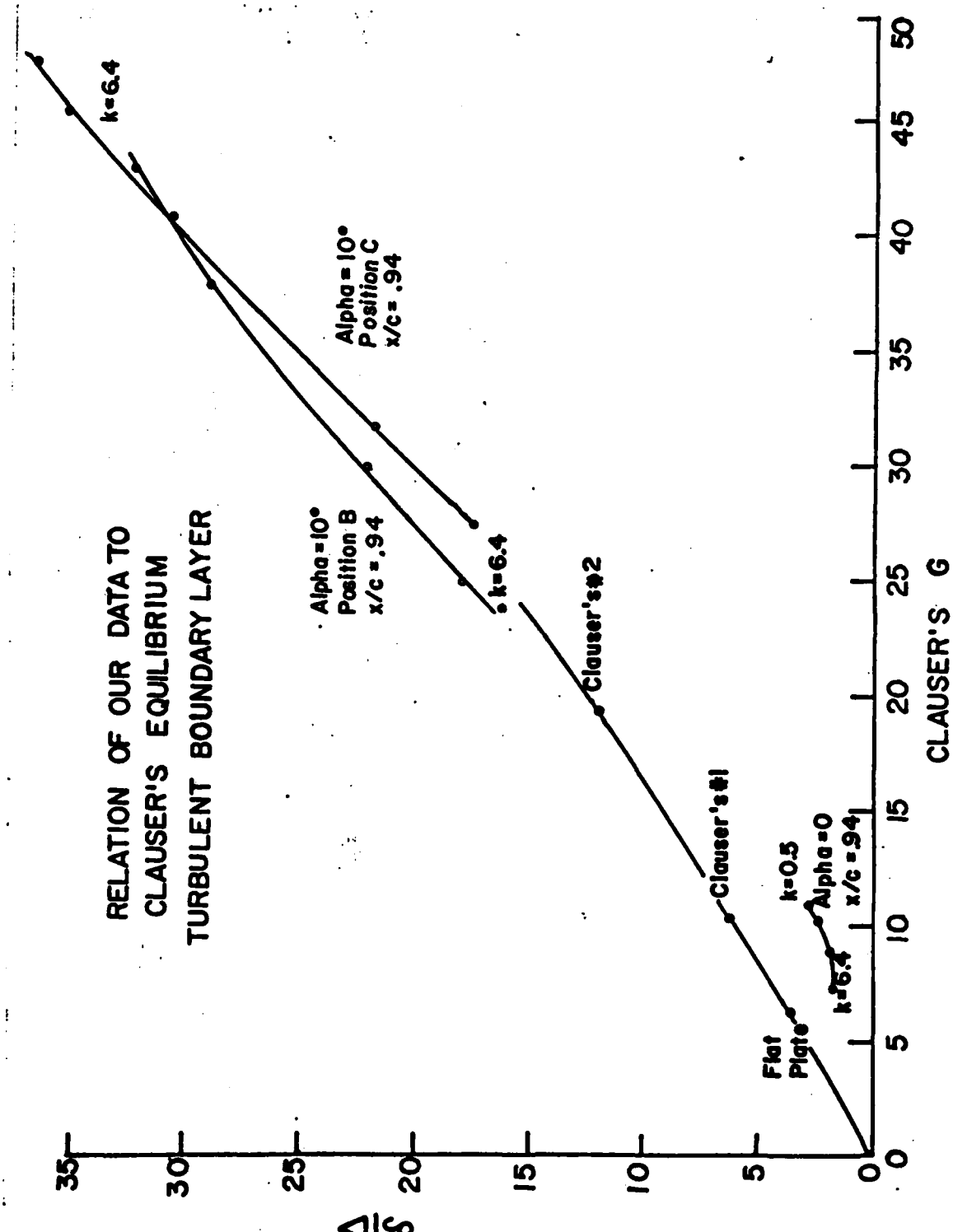

FIGURE 24: RELATION OF MEAN PROFILES TO SIMILARITY SOLUTION